NASA TECHNICAL NOTE

NASA TN D-1861

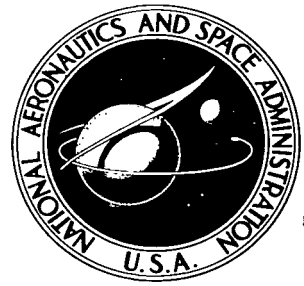

NASA TN D-1861

EXPERIMENTAL INVESTIGATION OF INSULATING REFRACTORY-METAL HEAT-SHIELD PANELS

by Gregory R. Wichorek and Bland A. Stein

Langley Research Center
Langley Station, Hampton, Va.

NATIONAL AERONAUTICS AND SPACE ADMINISTRATION • WASHINGTON, D. C. • DECEMBER 1964

EXPERIMENTAL INVESTIGATION OF INSULATING REFRACTORY-METAL HEAT-SHIELD PANELS

By Gregory R. Wichorek and Bland A. Stein

Langley Research Center
Langley Station, Hampton, Va.

NATIONAL AERONAUTICS AND SPACE ADMINISTRATION

For sale by the Office of Technical Services, Department of Commerce,
Washington, D.C. 20230 -- Price $3.00

EXPERIMENTAL INVESTIGATION OF INSULATING REFRACTORY-METAL HEAT-SHIELD PANELS

By Gregory R. Wichorek and Bland A. Stein
Langley Research Center

SUMMARY

The results of an experimental study to determine the capabilities and limitations of a thermal protection system utilizing thin-gage, refractory-metal shields are presented. Cyclic radiant-heating tests to 2,400° F (1,589° K) were performed on a heat-shield panel with molybdenum-alloy shields coated with a silicide-base coating, and a radiographic technique was used to detect oxidation damage and brittle cracking of the coated shields. A heat-shield panel with columbium-alloy shields was subjected to supersonic flow conditions at a Mach number of 3 and dynamic pressure of 1,500 lb/ft^2 (71.8 kN/m^2). The results of preliminary tests on a prototype panel with nickel-alloy shields subjected to radiant-heating and wind-tunnel conditions are also reported. Evaluation tests on the molybdenum-alloy shield material were made at temperatures ranging from room temperature to 2,900° F (1,866° K). Oxidation results and metallurgical studies covering diffusion phenomena for coated molybdenum-alloy coupons and small riveted configurations under continuous and cyclic conditions at temperatures to 2,900° F are also given.

INTRODUCTION

One structural design approach frequently proposed for aerospace vehicles is termed the hot-structure concept in which the structure operates near the equilibrium temperature and supports the applied loads (ref. 1). During reentry some areas of the primary structure may experience temperatures above the desired use temperature of the structural material unless protected from the high-temperature environment. For such areas, nonload-carrying heat shields with fibrous high-temperature insulation are generally used. The insulation maintains the primary structure within the useful temperature range of the material.

Metallic heat-shield designs generally utilize a lightweight outer skin. The major design problem involves the method of supporting the outer skin so that it will survive the dynamic loads and high-noise-level environments of exit and reentry and will accommodate the thermal expansion resulting from the large temperature differences between the shield and structure. Refractory metals are frequently considered for heat-shield applications because of their high melting points and their retention of strength above 2,000° F (1,366° K). However, those refractory metals presently being considered exhibit poor oxidation resistance

above 2,000° F and require the use of protective coatings to prevent degradation at these temperatures. The degradation of coated refractory metals under cyclic temperature exposure (ref. 2) has a direct bearing on the reusability of refractory-metal components in aerospace vehicles. Moreover, the life of the complex structural components has been shown in reference 1 to be less than the life of small coupons. Although considerable data are available in the literature on tests of coupons and small coated parts, data on tests of complete systems including heat shields, insulation, and structure are limited.

A study was undertaken to explore some of the capabilities and limitations of a thermal protection system utilizing coated molybdenum-alloy shields and a quartz-fiber insulation. The underlying structure was a panel representative of a structural skin for a reentry glider (ref. 3). The present paper describes the fabrication of the molybdenum-alloy shields and reports the results of cyclic radiant-heating tests on the heat-shield panel. Information was also obtained on the fabrication of columbium-alloy shields, and the performance of the thermal protection system with columbium-alloy shields subjected to supersonic airflow conditions is reported. In order to develop fabrication techniques and experimental procedures a prototype heat-shield panel with nickel-alloy shields was fabricated. The results of radiant-heating and wind-tunnel tests on the prototype panel are also reported herein.

This investigation includes the results of various tests to evaluate the properties of the coated molybdenum-alloy sheet. The tests included are tensile tests at room and elevated temperatures, continuous and cyclic oxidation tests on coupons and small riveted configurations at temperatures to 2,900° F (1,866° K), and metallurgical studies including diffusion phenomena and coating failure mechanisms. In addition, the results of tensile-shear tests on spot welds in the columbium-alloy sheet are presented.

The units used for the physical quantities in this paper are given both in the U.S. Customary units and in the International System of Units, SI (ref. 4). Appendix A is included for the purpose of explaining the relationships between these two systems of units.

SPECIMENS

Panels

Three heat-shield panels were used in the investigation. Each panel consisted of a corrugated outer skin or shield, a layer of insulation, and a primary structure. Three materials were used for the shields. The shield materials were molybdenum alloy (Mo-0.5Ti), columbium alloy (Cb-33Ta-1Zr), and nickel-base alloy. The molybdenum-alloy shields were coated with a columbium-modified silicide-base coating. The quartz-fiber insulation, Q-felt, and the primary structure, fabricated from the previously mentioned nickel-base alloy, were identical for all three panels. The panels are referred to hereinafter by their shield material.

The silicide-base coating is applied to molybdenum alloys in a single-cycle pack-cementation process. Specific details of the coating process are reported in reference 5. The coated shields and auxiliary specimens used in this investigation were received by the National Aeronautics and Space Administration during the latter part of 1961 and the first part of 1962.

Design.- Design details of the heat-shield panels are shown in figure 1. The shields, shield supports, and primary structure were fabricated from 0.010-inch- (0.025-cm-) thick sheet. The outer skin consisted of three overlapping sheets which were corrugated to a pitch of 0.75 inch (1.90 cm) and a depth of 0.060 inch (0.152 cm) as shown in figure 1(a). Shield supports were riveted to the molybdenum-alloy and nickel-alloy outer corrugated sheets and were spotwelded to the columbium-alloy outer corrugated sheets. The shields, the shield supports, and, where applicable, the rivets were made of the same material for each panel. The rivet design is shown in figure 1(b). This rivet was specifically designed to increase the gap between the supports and the outer corrugated sheet for better coating deposition as shown in figure 1(c). The spot-welded joints between the columbium-alloy supports and the outer corrugated sheet are shown in figure 1(d). The shield supports extended into slots machined in the channels which were spotwelded to the primary structure. (See figs. 1(a), 1(c), and 1(d).) Inconel rods, 0.093 inch (0.236 cm) in diameter and 19.8 inches (50.3 cm) long, were inserted into the channels and through the holes in the shield supports to attach the shields to the structure.

A quartz-fiber insulation was used between the shields and primary structure of the panels. The insulation was approximately 0.4 inch (1.0 cm) thick, and the density was approximately 4.3 lb/ft^3 (68.9 kg/m^3).

The primary structure consisted of a beaded sheet seam-welded to a corrugated sheet having 60°, 1/2-inch- (1.3-cm-) flat corrugations. (See fig. 1(a).) Z-stiffeners at each end of the corrugated sheet were seamwelded to the beaded sheet and blind riveted to the bottom flats of the corrugations. The primary structure was representative of the skin panel used in the investigation of a hot structure for lifting reentry vehicles (ref. 3).

Fabrication.- Most of the operations used to fabricate the molybdenum-alloy shields and supports could not be performed at room temperature because small cracks developed in the sheet material. Shearing, forming, drilling, and dimpling were accomplished by preheating the material, and in some cases the tooling, to 300° F (422° K) or 500° F (533° K). In addition, the forming operation had to be performed in the cross-grain direction of the molybdenum-alloy sheet. Riveting of the shield supports to the corrugated sheets was accomplished by using a die heated to 800° F (700° K). Smooth edges were obtained on the corrugated sheets and shield supports by hand sanding and machine tumbling, respectively. The operations required to fabricate the columbium-alloy shields, as well as the nickel-alloy shields and primary structures, were readily performed. However, the single spot welds joining the columbium-alloy shield supports to the corrugated sheets were limited in diameter to approximately 0.055 inch (0.140 cm) because of the design of the shield and shield supports.

The molybdenum-alloy rivets, shield supports, and corrugated sheets were coated with a silicide-base coating before and after assembly. The construction

of the shield is such that it provides a severe test of the oxidation-protective coating. Inspection of the coated molybdenum-alloy shields revealed that some distortion occurred. This distortion changed the pitch of the corrugations. In some portions of the corrugated sheet the pitch was greater and in other portions less than the fabricated dimension. As a result of this distortion, the shield supports were not alined with the slots in the structural channels. Before the shields could be attached to the structure, widening of the slots in the channels was necessary.

Two pieces were broken from a molybdenum-alloy corrugated sheet during the riveting operation. At these damaged areas some material was removed from the corrugated sheet to eliminate cracks. One of the damaged areas in the corrugated sheet was covered with a patch which was corrugated to match and overlap the sheet corrugations. (See fig. 2.) The patch contained three riveted supports for attachment to the structure. The entire patch received one coating application. The other damaged area consisted of a V-notch along the edge of the outer corrugated skin and resulted in the elimination of one shield support. The repaired edges of the molybdenum-alloy corrugated sheet were protected with a single coating application.

Auxiliary Specimens

Tensile specimens for mechanical property tests were fabricated from annealed columbium-alloy and arc-cast stress-relieved molybdenum-alloy sheets, nominally 0.010 inch (0.025 cm) thick. The molybdenum-alloy specimens utilized in the present investigation were obtained from the same lot procured for the studies reported in references 2 and 6. Some of the molybdenum-alloy specimens were coated with the silicide-base coating to determine the properties of the coated sheet. The silicide-base coating investigated herein is designated as coating F in references 2 and 6. The tensile specimens were 6 inches (15.2 cm) long and 0.50 inch (1.27 cm) wide with a 4-inch (10.2-cm) gage section reduced to 0.375 inch (0.953 cm).

Tensile-shear specimens were made from the columbium-alloy sheet material to determine shear strength of resistance spot welds. To fabricate the specimens, two sheets 1/4 inch (0.635 cm) wide and 1 inch (2.54 cm) long were overlapped 1/4 inch and a single resistance spot weld was made at the center of the overlapped area.

Oxidation coupons were fabricated from the molybdenum-alloy sheet as described in reference 2. The edges were rounded by machine tumbling prior to coating. The coupons were both single and double coated with the silicide-base coating.

Specimens of two configurations were fabricated of molybdenum alloy to determine the problems involved in coating riveted assemblies. These configurations will hereinafter be referred to as sheet-V specimens and sheet-Z specimens and are shown, respectively, in figures 3(a) and 3(b). The V-shaped clip of the sheet-V specimens and the rivets of the sheet-Z specimens were fabricated from molybdenum-alloy wire 1/8 inch (0.318 cm) in diameter. The ends of the V-clips were machined to serve as rivet heads so that the V-clips could be riveted to

the sheets. The rivets of the sheet-Z specimens were identical to those used on the molybdenum-alloy heat-shield panel. The forming, drilling, and machining operations required to fabricate these specimens were performed at temperatures from 300° F (422° K) to 500° F (533° K). The single-coated sheet-V and sheet-Z specimens were riveted uncoated at 800° F (700° K) to 1,000° F (811° K) and then a single coat of the silicide-base coating was applied. The separate components of the double-coated specimens were first coated by the coating supplier before assembly. Then the sheet-Z specimens were riveted at 800° F to 1,000° F and the sheet-V specimens were riveted at approximately 2,000° F (1,366° K). After assembly, the specimens were given a second application of the silicide-base coating.

EQUIPMENT AND PROCEDURES

Panel Tests

Radiant-heating tests.- The radiant-heating tests were accomplished with a quartz-lamp radiator, approximately 28 inches (71 cm) by 29 inches (74 cm), shown in figure 4. The lamps were mounted in grooves machined in a water-cooled aluminum reflector. Three-phase electrical power was distributed to the lamps from an ignitron power supply. Power was controlled by a computer which continuously compared outer-skin temperature response with a programed temperature-time curve.

The temperature-time histories applied to the shields of the nickel-alloy and molybdenum-alloy panels are shown in figure 5. The nickel-alloy panel was subjected to one heating cycle with a platinum/platinum—13-percent-rhodium thermocouple spotwelded to the outer skin for temperature control. The molybdenum-alloy panel was subjected to five heating cycles with a spring-loaded platinum/platinum—13-percent-rhodium thermocouple probe contacting the coated outer skin for temperature control. The contacting thermocouple probe was developed and used because direct attachment of thermocouples to coated metals may result in damage to the coating and/or temperature-response problems. The design, mounting, and temperature response of the thermocouple probes are discussed in appendix B. Nine probes were used to measure temperature distributions on the coated molybdenum-alloy shields. Temperature distributions were measured on the nickel-alloy shields and primary structure with spotwelded chromel-alumel thermocouples. The thermocouple output signals were recorded on magnetic tape in the Langley Central digital data recording facility. The recording and readout accuracy is approximately 0.1 percent of full-scale signal.

A radiographic inspection technique was developed to ascertain the effectiveness of the protective coating and the structural integrity of the molybdenum-alloy panel. Radiographs were taken with a 200-kva or a 110-kva portable X-ray machine. The X-ray machine was positioned directly over the panel and also at an angle to the panel. Complete coverage of the panel was obtained by taking a series of overlapping radiographs at each machine position. The molybdenum-alloy panel was X-rayed after assembly and after every heating cycle.

Wind-tunnel tests.- The nickel-alloy and columbium-alloy panels were tested under aerodynamic conditions in the Langley 9- by 6-foot thermal structures tunnel. The heat-shield panels were mounted in a panel holder at an angle of attack of 0°. (See fig. 6(a).) Airflow was at Mach number 3 with a stagnation temperature of 450° F (505° K), and the maximum temperature experienced by the panels was approximately 300° F (422° K). The nickel-alloy panel was subjected to stable free-stream dynamic pressures of 1,500 lb/ft^2 (71.8 kN/m^2) and 2,500 lb/ft^2 (120 kN/m^2) and the columbium-alloy panel was subjected to a stable free-stream dynamic pressure of 1,500 lb/ft^2. The panels were alined with the outer-skin corrugations first parallel and then perpendicular to the airstream at each dynamic pressure. The tunnel conditions were maintained for approximately 60 seconds. Sliding doors on the panel holder protected the panels from severe random pressure fluctuations which occur during tunnel starting and shutdown periods. (See fig. 6(a) and ref. 7.) After the doors were opened, the pressure differential across the specimen was maintained at less than 1/4 psi (1.72 kN/m^2) by means of an adjustable port on the panel holder.

Cameras and deflectometers were used to detect and record motion of the shields. Grid lines painted on the outer skin of the panels (fig. 6(a)) aided in the visual detection of motion. The cameras were operated at 750 and 250 frames per second. Six deflectometers were bolted to a heavy steel bar attached to the panel mounting frame to detect motion of the shields as shown in figure 6(b). The deflectometers were mounted 3/16 inch (0.476 cm) beneath the outer skin of the panel through $1\frac{1}{8}$-inch (2.86-cm) holes in the primary structure and insulation. The inductance-type deflectometers are flat wire coils that are coupled by their electrical field with the resistance of the outer skin material to produce an electrical signal. The output signal limited the measurement of shield motions to inward deflections of 1/8 inch (0.318 cm) and to outward deflections of 1/16 inch (0.159 cm).

Auxiliary-Specimen Tests

Metallurgical examinations.- The metallurgical examinations consisted of microscopic examinations of sectioned specimens, X-ray diffraction studies of the surfaces and the various layers of the coating for as-coated and tested specimens, X-ray emission studies of the surface of as-coated and tested specimens, and microhardness measurements of the molybdenum-alloy substrate before coating, as-coated, and after testing. Specific details of the procedures used for microscopic examinations, X-ray diffraction, and microhardness measurements are presented in reference 6. The X-ray emission studies were performed with a diffractometer; both platinum K_α and chromium K_α radiation were utilized. All microhardness data were obtained by using a Knoop indenter with a 0.1-kilogram load.

Tensile and tensile-shear tests.- The room-temperature tensile stress-strain tests to determine mechanical properties and the tensile-shear tests to determine the strength of the resistance spot welds were performed in a 120,000-pound- (534-kN-) capacity universal hydraulic testing machine at the Langley Research Center. The tensile and tensile-shear tests were performed

at nominal strain rates of 0.005 per minute (0.000083 per second) to yield and 0.050 per minute (0.00083 per second) from yield to failure and the tensile-shear tests, at 0.005 per minute to failure. Strain rates were controlled by continuously monitoring head motion during the test. In the tensile tests, strains were measured by use of optical strain gages attached to both sides of the specimen; strains were read while the strain rate was maintained.

High-temperature tensile tests were performed in a 10,000-pound- (44.5-kN-) capacity screw-driven testing machine at the Langley Research Center at the same strain rates used for the room-temperature tensile tests. For high-temperature strain determinations, the head motion of the screw-type machine was calibrated to give a direct indication of specimen strain. The calibration was accomplished as follows: The tensile specimen was first stressed to 20 ksi (138 MN/m^2) at room temperature. The resulting head motion was converted to strain on the basis of Young's modulus previously established with the aid of the optical strain gages. This strain calibration was then used in the elevated-temperature tests. The 20 ksi applied to the specimen at room temperature was determined to be within the elastic limit of the material. Specimens were heated by resistance-heating techniques. Temperatures were measured with an optical pyrometer at a wavelength of 0.65 micron (0.65 μm), assuming a coating emissivity of 0.8. Specimens were exposed to the test temperature for 6 minutes (360 seconds) before loading. For all tensile tests, elongation measurements were made by using finely scribed pencil lines at 1/4-inch (0.635-cm) intervals along the specimen.

Oxidation tests.- Details of the equipment used for the oxidation tests are described in reference 2. The tests were performed at temperatures from 1,450° F (1,061° K) to 2,900° F (1,866° K). Coupons were subjected to continuous and cyclic tests. Riveted configurations were subjected to cyclic tests only. The three cyclic test conditions, hereinafter referred to as 1.0-hour, 0.1-hour, and 0.5-1.0-0.5-hour cycles, are also described in reference 2. Failure of the coating was determined by a 10-percent weight loss in the specimen due to the formation of the volatile MoO_3 at the test temperature.

RESULTS AND DISCUSSION

Panels

Heat-shield design.- The shields were designed with a corrugated outer skin because a corrugated sheet can expand and contract under relatively small forces in the transverse direction and because a corrugated skin provides the necessary stiffness to transmit aerodynamic loads and to resist flutter when adequately supported (ref. 7). Rotation of the shield supports and bending of the outer skin in the vicinity of the attachments accommodates expansion and contraction in the longitudinal direction. The design of the shield supports and their attachment to the outer skin and primary structure provided a relatively continuous outer surface. Other heat-shield designs may utilize either threaded fasteners at the outer skin or access holes in the outer skin for internal attachment. Threaded fasteners at the outer skin (ref. 7) would require the use of coated refractory-metal screws to assemble the shields to the primary

structure. During assembly the coating on the screws may be damaged, necessitating coating repair or limited reuse of the fasteners. Access holes in the outer skin may disturb the aerodynamic flow over the outer skin and may also lead to a flow of heat into the panel through the access holes. Reliable plugging of the access holes presents difficult design problems and also increases the heat-shield weight.

Several difficulties were encountered in assembling the test panels with the selected shield attachment technique. Bending of the ductile nickel-alloy and columbium-alloy supports and cracking or breaking of the brittle molybdenum-alloy supports occurred when the supports were not properly alined with the slotted channels. Alinement of the shield supports in the appropriate slots was difficult because the length of the corrugated skins in the transverse direction resulted in excessive flexibility for assembly. The most satisfactory method found for assembly of the heat-shield panels consisted of first attaching the shields to the primary structure and then inserting the insulation between the shields and structure. Insertion of the insulation was accomplished by placing the insulation between two thin metal sheets, sliding the sheets together with the insulation between the outer skin and primary structure, and removing the thin metal sheets when the insulation was properly positioned.

The thermal protection weights for the molybdenum-alloy, columbium-alloy, and nickel-alloy panels are given in table I. The thermal protection weights for the molybdenum-alloy and columbium-alloy panels were approximately 1.1 lb/ft^2 (53 N/m^2) and 1.0 lb/ft^2 (48 N/m^2), respectively, and compare favorably with a frequently quoted requirement of 1.0 lb/ft^2 for a lifting reentry vehicle. The quartz-fiber insulation was only 14.5 percent of the total thermal protection weight of the molybdenum-alloy panel. The weights of all three heat-shield panels could be reduced by replacing the inconel rods with tubing. The weight of the primary structure, representative of the structural skin of a lifting reentry vehicle, was approximately 1.1 lb/ft^2.

Radiant-heating tests.- The nickel-alloy panel was utilized to evaluate the performance of the heat-shield design under radiant heating. The specimen was subjected to one heating cycle with a maximum temperature of 2,100° F (1,422° K) on the shields. (See fig. 5.) The panel rested on four point supports under a bank of quartz lamps. No other support or restraint was provided for the panel. After the heating test, the nickel-alloy outer skins were permanently buckled between rows of shield supports in the direction of the corrugations as seen in figure 7; the buckle shape was characteristic of wide column buckling. However, neither the shield supports nor the riveted joints were damaged. The outer skins act essentially like thin plates restrained at two edges by the supports. Loading and buckling of the skins result from the difference in thermal expansion between the shields and the primary structure. The buckles in the shield probably occurred because of the low strength of the material at the test temperature, yield stress of 4 ksi (27.6 MN/m^2) at 2,000° F (1,366° K), and low modulus of elasticity of 6×10^6 psi (41.4 GN/m^2) at 2,000° F. However, the design was believed to be adequate for the molybdenum-alloy panel because of the higher yield strength of 12 ksi (82.8 MN/m^2) and higher elastic modulus of 11×10^6 psi (75.8 GN/m^2) at the test temperature of 2,400° F (1,589° K). In

addition, the linear thermal expansion of the molybdenum alloy at 2,400° F is approximately one-half of that for the nickel alloy at 2,000° F.

The molybdenum-alloy panel was subjected to five radiant-heating cycles with a maximum temperature of 2,400° F on the shields. (See fig. 5.) The temperature distribution measured through the panel at the center of the panel is shown in figure 8. The channel which supported the shield reached a peak temperature of 1,730° F (1,217° K). The beaded sheet or outer skin of the primary structure experienced a maximum temperature of 1,510° F (1,094° K). There was a temperature difference of 350° F (194° K) from the top to the bottom of the structural corrugations. The outer skin of the primary structure was heated to 1,130° F (883° K) midway between channels along the center line of the panel. At this point the temperature difference between the top and bottom of the structural corrugations was 135° F (75° K). The test data show that the thermal protection system maintained the primary structure below 1,600° F (1,144° K); this temperature is within the useful temperature range of the material for this application.

The primary structure was warped after the first heating cycle. Further distortion of the structure was not evident after the succeeding cycles. Bowing of the primary structure was greater perpendicular to the corrugations than it was parallel to the corrugations. Based on the results of loading and heating tests performed on a similar structure fabricated from another nickel-alloy material (ref. 3), distortion of the primary structure perpendicular to the corrugations may be reduced or eliminated by increasing the thickness of the Z-stiffeners.

An average temperature-time history was computed for the primary structure of the molybdenum-alloy panel and is shown in figure 9. The heating-rate input to the panel was determined from the programed temperature-time history of the shields. The heat-shield panel was divided into layers and the general heat-balance equation was written in terms of finite differences with the assumptions of one-dimensional heat flow, conduction through the insulation and supports, heat absorption, and heat losses from the primary structure by radiation and convection. The heat capacity and the variation of thermal conductivity with temperature of the layers were included in the equations which were solved by an iterative method on an electronic computer. The experimental temperature response of the primary structure shown in figure 9 is an average of the temperatures measured on the outer skin of the structure. Figure 9 shows that during the first 660 seconds of heating the experimentally determined temperature rise of the primary structure was less than the calculated temperature rise. The thermal resistance of the connections between the shields and primary structure may have been greater experimentally than calculated because contact resistance at the connections was not taken into account. Such an increase in thermal resistance would decrease the temperature response of the primary structure, as indicated by the experimental curve, since the primary mode of heat transfer during this time was conduction through the shield supports. Figure 9 also shows that the experimental temperature curve was lower than the calculated curve during the cooling portion of the cycle. This difference may have resulted from the experimental heat losses being greater than the theoretical heat losses because of higher radiation and convection losses from the structure.

The effectiveness of the silicide-base coating in protecting the molybdenum-alloy shields from oxidation was determined by radiographic inspection of the molybdenum-alloy panel after every heating cycle. Damage to the panel was clearly indicated on the radiographs by a change in density of the affected area as shown in figure 10. However, detection of damage was difficult or impossible when the X-rays had to penetrate large thicknesses or when several components were superimposed. A series of radiographs were taken from directly above the panel to detect damage to the shields and, to some degree, damage to the shield supports. (See fig. 10(a).) The series of radiographs taken at an angle to the panel were used to detect damage to the shield supports. (See fig. 10(b).) The validity of radiographic detection of damage is shown in figure 11. Figure 11(a) is a photograph showing no visible damage to a coated molybdenum-alloy shield after five heating cycles. A radiograph taken of this same area (fig. 11(b)) indicates oxidation of the molybdenum-alloy shield. When the coating was removed at the areas indicated by the radiograph to be damaged, oxidation of the molybdenum alloy was evident as shown in figure 11(c).

The cyclic deterioration of the coated molybdenum-alloy shield supports is shown in figure 12. It should be noted that the percentage of damaged supports shown in the table does not indicate complete failure or the inability of the supports to carry load. Five percent of the shield supports were damaged during the assembly of the panel because of the brittle behavior of the material. After the first heating cycle, an additional 26 percent of the shield supports were damaged. The majority of these failures were at the holes, bends, and rivets - areas of maximum stress. Excessive bending of the coated supports as a result of the difference in thermal expansion between the outer skin and primary structure may have caused these failures. Also, the failures may have been accelerated due to the susceptibility of these areas to edge failures (ref. 2).

Coating failures along the edges of the outer skins occurred during the first heating cycle. Based on the results of the cyclic-heating tests performed on the small riveted configurations, these edge failures were considered to be premature. Damage to the coating along the edges of the outer skins may have occurred during the assembling, X-raying, and mounting of the panel for testing. Consequently, the need for extreme care in the handling of coated specimens is indicated. Coating failures on the surface of one of the outer skins occurred during the second heating cycle. No surface failures were detected on the other two outer skins after five heating cycles. Radiographs indicating the growth of oxidized regions on the coated molybdenum-alloy shields are shown in figure 13.

Wind-tunnel tests.- Wind-tunnel tests were performed on the columbium-alloy and nickel-alloy panels with the outer skin corrugations alined first parallel and then perpendicular to the airstream at each dynamic pressure. The shields of both panels experienced some oscillatory motions when the protective doors were opened and closed, but these motions were short lived.

The columbium-alloy panel was subjected to a free-stream dynamic pressure of 1,500 lb/ft^2 (71.8 kN/m^2). The shields experienced some overall motion at both orientations, but the shields did not flutter during the stable tunnel conditions. After the tunnel tests, examination of the panel revealed no damage to the corrugated outer skin, the shield supports, or the spot welds joining the supports and the outer skin. The overall motion of the columbium-alloy shields

may have been due to the flexible shield supports and the relatively low modulus of elasticity of 17×10^6 psi (117 GN/m^2) for the columbium alloy.

After a radiant-heating test, the nickel-alloy panel was subjected to free-stream dynamic pressures of 1,500 lb/ft^2 (71.8 kN/m^2) and 2,500 lb/ft^2 (120 kN/m^2). There was no detectable motion of the shields at either orientation at each dynamic pressure. The panel withstood the stable tunnel conditions without flutter or any damage. The greater stability of the nickel-alloy shields may have been due to the higher modulus of elasticity of 32×10^6 psi (221 GN/m^2) for the material and, to some extent, to permanent buckles formed in the shields during the radiant-heating test.

Auxiliary Specimens

Mechanical-property tests.- The arc-cast molybdenum-alloy sheet used in this investigation was supplied in the stress-relieved condition. This material has a Knoop hardness of 398 (fig. 4 of ref. 6) and a recrystallization time of 1 hour at 2,400° F (1,589° K). Typical photomicrographs of the molybdenum-alloy sheet before coating and in the as-coated condition are shown in figure 14. Figure 14(b) shows that a central zone along the midplane of the sheet has been recrystallized by the coating procedure. Approximately 40 percent of the substrate has been recrystallized. Microhardness indentations in the recrystallized and unrecrystallized zones gave uniform Knoop hardnesses of 252 and 361, respectively. The average Knoop hardness, 317, of the as-coated substrate was taken in this case as a weighted average of the values in the recrystallized and unrecrystallized zones. Substrate hardness values for coated molybdenum-alloy sheet were uniform through the thickness for specimens tested at 2,400° F to 2,900° F (1,866° K). Hardness values for the recrystallized and unrecrystallized zones in the as-coated material and the specimens tested at 2,000° F (1,366° K) were also uniform but of different magnitudes. The variation of substrate hardness with exposure time and temperature is shown in figure 15.

Reference 8 indicated that the hardness of the molybdenum-alloy substrate can be raised as much as 200 Knoop numbers below a large crack in the coating as a result of the penetration of atmospheric gases into the substrate. No such increase was found on the specimens exposed in this investigation to temperatures from 2,000° F (1,366° K) to 2,900° F (1,866° K), an indication that the silicide-base coating prevented embrittling atmospheric gases from entering the substrate until the coating failed.

The room-temperature mechanical properties of the as-received molybdenum-alloy sheet, determined from tensile stress-strain tests, are given in table II. The results of tensile tests on the molybdenum-alloy sheet coated with the silicide-base coating at room and elevated temperatures are presented in table III. The tensile properties of the coated molybdenum-alloy sheet are compared in figure 16 with similar data from reference 9 for molybdenum-alloy sheet coated with another silicide-base coating. Figure 16 shows close agreement between the tensile properties of the coated molybdenum-alloy sheets, with the exception of room-temperature yield stress. This difference exists probably because the molybdenum-alloy sheet was recrystallized less than 5 percent by the

coating process of reference 9 whereas the molybdenum-alloy sheet was recrystallized 40 percent by the coating process in the present study. For heat-shield applications, usable tensile properties are retained for molybdenum-alloy sheet coated with the silicide-based coating at temperatures to 2,900° F (1,866° K), provided the coating is not damaged. However, possible brittle behavior of molybdenum-alloy sheet at low temperatures after recrystallization must also be considered.

The room-temperature mechanical properties of the annealed columbium-alloy sheet determined from tensile stress-strain tests are given in table IV. The tensile-shear tests of the single columbium-alloy spot welds gave an average failure load of 102 pounds (454 N). Failure occurred by shearing through the diffusion-type spot weld. Photomicrographs of a representative spot weld in the columbium-alloy sheets are shown in figure 17. The average diameter of the spot welds was approximately 0.055 inch (0.140 cm). If it is assumed that the ultimate shear stress of the material ranges from 0.55 to 0.60 of the ultimate tensile stress, the shear strength of the spot welds was 94 to 100 percent of the ultimate shear strength of the base metal. These data indicated that the columbium-alloy spot welds were adequate for the heat-shield design of this investigation.

Oxidation tests.- The various phases detected in the silicide-base coating are presented in appendix C. During high-temperature exposures in air, a thin layer of protective glass (SiO_2) is formed on the surface of the specimen to provide oxidation resistance (refs. 2 and 6). In the present investigation the crystalline form of glass, cristobalite, was found in appreciable concentrations in all failed specimens after continuous tests and in higher concentrations after cyclic tests. In the specimens that were exposed at temperatures from 2,000° F (1,366° K) to 2,900° F (1,866° K) and did not fail, cristobalite was either absent entirely or present in considerably smaller quantities than in the failed specimens. It therefore appears that the failure mechanisms presented for silicide-base coatings on molybdenum-alloy sheet at 2,500° F (1,644° K) in reference 2 are applicable to the silicide-base coating on molybdenum-alloy sheet at temperatures from 2,000° F to 2,900° F.

The results of oxidation tests on the molybdenum-alloy coupons coated with the silicide-base coating are presented in table V. Some of the data were previously presented in reference 2, where the coating investigated herein is designated as coating F. Failure occurred first at edges for more than 50 percent of the coupons in the continuous tests and for more than 90 percent of the coupons in the cyclic tests. Coating lifetimes for single- and double-coated coupons exposed to continuous and 1.0-hour cyclic tests are plotted in figure 18. This figure shows that scatter in the cyclic-test data is more evident than in the continuous-test data. The double-coated coupons had longer lifetimes than the single-coated coupons at both 2,000° F (1,366° K) and 2,500° F (1,644° K). The double- and single-coated coupons had approximately the same lifetimes at 2,700° F (1,755° K). This may be explained by a decrease in viscosity of the SiO_2 layer at the higher temperatures, providing for better "self-healing" characteristics. Another factor may be an increase in the initial rate of formation of the SiO_2 layer at the higher temperatures. Figure 19 clearly indicates a reduction in the performance of the silicide-base coating under

cyclic conditions at 2,500° F. This figure also shows that double-coated coupons have much longer lifetimes than single-coated coupons under continuous and cyclic exposures at 2,500° F.

The results of 1.0-hour cyclic oxidation tests on the coated sheet-V and sheet-Z specimens fabricated from the molybdenum alloy are presented in table VI. The coating life of the riveted configurations and the coupons subjected to 1.0-hour cyclic tests are compared in figure 20. Where there was visual evidence of oxidation damage on these specimens, the damage was generally observed after the last or next to the last heating cycle. The single-coated sheet-V and sheet-Z specimens generally exhibited shorter lifetimes than the single-coated coupons, as might be expected. However, the double-coated riveted specimens not only had shorter lifetimes than the double-coated coupons but they also had shorter lifetimes than the single-coated riveted specimens. Therefore, the double-coated riveted specimens may be said to have failed prematurely at all test temperatures from 2,000° F (1,366° K) to 2,900° F (1,866° K). The appearance of sheet-V and sheet-Z specimens before and after 1.0-hour cyclic tests is shown in figures 21 and 22, respectively. In general, the single-coated riveted specimens failed at the rivet, at the edge of the sheet, or in both areas simultaneously. All the double-coated specimens failed at riveted joints. Apparently the riveting operation had severely damaged the first coating and the second coating application did not adequately repair the damaged areas. The test results indicate that the coating of riveted components after fabrication provides better oxidation protection than the precoating, fabrication, and recoating of riveted components.

Diffusion.- The average reduction in substrate thickness for a single application of the silicide-base coating was approximately 0.0016 inch (0.00406 cm), and the average coating thickness was 0.0019 inch (0.00483 cm).

Diffusion of silicon into the molybdenum-alloy substrate occurs when the coating is exposed to high temperatures in air. The various coating phases which form are discussed in appendix C. The loss of substrate thickness due to diffusion is presented in table VII and shown as symbols in figure 23. The curves were obtained by cross-plotting the test data of substrate loss against temperature and were smoothed to give the best possible fit. Although the data show scatter within the test temperatures, the curves give an indication of substrate loss with increasing time and temperature. It is realized that the diffusion mechanisms which operate may change within the time and temperature ranges shown. Most important, the data indicate that solid-state diffusion may be a serious problem when thin-gage molybdenum-alloy sheet coated with the silicide-base coating is used at temperatures from 2,400° F (1,589° K) to 2,900° F (1,866° K).

CONCLUDING REMARKS

This study was made to investigate the capabilities and limitations of a thermal protection system utilizing thin-gage refractory-metal shields. The following comments and conclusions are based on this experimental study:

1. The thermal protection system utilizing coated molybdenum-alloy shields at 2,400° F (1,589° K) maintained the primary structure within its useful temperature range.

2. The thermal protection weights of the columbium-alloy and coated molybdenum-alloy heat-shield panels were approximately 1.0 and 1.1 lb/ft^2 (48 and 53 N/m^2), respectively. These weights compare favorably with a frequently quoted requirement of 1.0 lb/ft^2 for a lifting reentry vehicle.

3. The columbium-alloy heat-shield panel withstood a free-stream dynamic pressure of 1,500 lb/ft^2 (71.8 kN/m^2) in a Mach 3 wind tunnel.

4. Improvement of procedures for coating large thin-gage corrugated sheets is needed to prevent distortion of the corrugations. It appears that designs utilizing refractory-metal sheets should preferably consist of small rather than large pieces to minimize distortions.

5. Radiographic methods appear well suited for the detection of damage on coated molybdenum-alloy shields of complex design.

6. Care in the handling of coated components is needed to help overcome premature edge failures.

7. Oxidation damage was evident after fewer heating cycles on the large double-coated shields than on either the double-coated coupons or the double-coated riveted configurations.

8. The coating life of the double-coated riveted configurations was shorter than that of the single-coated specimens in cyclic temperature exposures at all temperatures from 2,000° F (1,366° K) to 2,900° F (1,866° K).

9. Cyclic exposures at temperatures of 2,500° F (1,644° K) and below severely lowered the oxidation protection of the silicide-base coating based on the average test values. At 2,700° F (1,755° K), both cyclic- and continuous-exposure specimens had approximately the same lifetimes.

10. Usable tensile properties were retained by the molybdenum-alloy sheet coated with the silicide-base coating for heat-shield applications up to 2,900° F (1,866° K). The coating apparently prevented embrittling atmospheric gases from entering the substrate until coating failure.

11. Solid-state diffusion of the coating into the substrate may be a serious problem when thin-gage molybdenum-alloy sheet coated with the silicide-base coating is used at temperatures from 2,400° F (1,589° K) to 2,900° F (1,866° K).

Langley Research Center,
National Aeronautics and Space Administration,
Langley Station, Hampton, Va., June 30, 1964.

APPENDIX A

CONVERSION OF U.S. CUSTOMARY UNITS TO SI UNITS

The International System of Units (SI) was adopted by the Eleventh General Conference on Weights and Measures, Paris, October 1960, in Resolution No. 12 (ref. 4). Conversion factors required for units used herein are:

Length: Inches × 0.02540 = Meters (m)

Time: Minutes × 60 = Seconds (s)

Temperature: $5/9\ (^{\circ}F + 459.7) = {}^{\circ}K$

Temperature difference: $\Delta(^{\circ}F) \times 5/9 = \Delta(^{\circ}K)$

Force: Pounds × 4.448 = Newtons (N)

Unit loading: Pounds per inch × 175.1 = Newtons per meter (N/m)

Density: Pounds per cubic foot × 16.02 = Kilograms per cubic meter (kg/m^3)

Unit weight: Pounds per square foot × 47.88 = Newtons per square meter (N/m^2)

Stress: Pounds per square inch × 6.895×10^3 = Newtons per square meter (N/m^2)

Pressure: Pounds per square foot × 47.88 = Newtons per square meter (N/m^2)

Prefixes to indicate multiples of units are:

giga	(G)	10^9
mega	(M)	10^6
kilo	(k)	10^3
centi	(c)	10^{-2}
milli	(m)	10^{-3}
micro	(μ)	10^{-6}

APPENDIX B

THERMOCOUPLE PROBE

Spring-loaded thermocouple probes were used to measure and control the temperature of the coated molybdenum-alloy shields. The probe components and assembly are shown in figure 24. The No. 30 gage platinum/platinum—13-percent-rhodium thermocouple wire was spotwelded to a 0.005-inch- (0.0127-cm-) thick thoriated-nickel disk. The thermocouple probes used on the molybdenum-alloy panel were installed with the springs compressed 5/8 inch (1.59 cm). The probes contacted the underside of the shields through 1/4-inch (0.635-cm) holes in the primary structure and insulation. A flat plate beneath the specimen supported the probes. (See fig. 25.)

The thermocouple probes were calibrated with a heat-shield panel representative of the molybdenum-alloy panel. The shields and primary structure of the representative panel, fabricated from the nickel alloy were identical in design to the molybdenum-alloy panel except for the shield supports. The representative panel was subjected to the same temperature-time conditions as the molybdenum-alloy panel. The thermocouple probes were installed for the calibration tests as previously described. Platinum/platinum—13-percent-rhodium thermocouples were spotwelded to the shields approximately 1/4 inch (0.6 cm) from the probe junctions as "standards" to measure the temperature response of the shields. Probe temperature response is compared with shield temperature response in figure 26. The temperature measured by the probe is lower than the shield temperature because of heat conduction from the probe junction along the thermocouple wire and contact resistance between the probe junction and the shield. Figure 26 also shows the average temperature difference between the shield and probe measurements. The maximum temperature deviations from the average temperature curve are $+30^{\circ}$ F ($+17^{\circ}$ K) and -35° F (-19° K). The representative panel was subjected to three heating cycles to obtain the data. The thoriated-nickel disks and the fibrous insulation behind the disks were replaced after each cycle.

APPENDIX C

IDENTIFICATION OF COATING PHASES

For the specimens in the as-received condition, X-ray diffraction data indicated the coating to be $MoSi_2$ with a thin region of Mo_5Si_3 adjacent to the coating substrate interface. The small amount of columbium added to the coating pack was not detectable in the coating by the X-ray diffraction methods. X-ray emission studies revealed a small percentage of iron on the specimen surface, but no columbium. In this case, however, the columbium peaks in the record may have been masked by the large molybdenum peaks obtained.

Formation of a thin layer of protective glass (SiO_2) on the surface of the specimen and diffusion of silicon into the molybdenum-alloy substrate occurs during high-temperature exposures in air as discussed in references 2 and 6. These phenomena are illustrated in figure 27. The thin layer of glass on the outer surface of the specimen is not visible in the photomicrographs but is evident on visual inspection of the specimens after high-temperature tests. In figure 27(a), it may be seen that diffusion of silicon into the substrate during the 1.0-hour exposure at 2,900° F (1,866° K) has resulted in the formation of a wide band of Mo_5Si_3 adjacent to the substrate at the expense of the $MoSi_2$. A thin band of Mo_5Si_3 at the outer surface, which formed as a result of the formation of SiO_2, is also evident (ref. 6). The "optical activity" of the $MoSi_2$ is visible in the polarized-light photomicrograph of figure 27(a). After longer exposures (fig. 27(b)) the lower silicide of molybdenum Mo_3Si is evident both at the coating-substrate interface as a result of diffusion and at the outer surface as a result of glass formation. These phenomena occurred at all temperatures investigated; the rate of formation of the lower silicide was proportional to exposure time and temperature.

REFERENCES

1. Mathauser, Eldon E.: Research, Design Considerations, and Technological Problems for Winged Aerospace Vehicles. Proceedings of the NASA-University Conference on the Science and Technology of Space Exploration, Vol. 2, NASA SP-11, 1962, pp. 499-510. (Also available as NASA SP-28.)

2. Rummler, Donald R., Stein, Bland A., and Pride, Richard A.: A Study of Several Oxidation-Resistant Coatings on Mo-0.5Ti Alloy Sheet at 2,500° F. NASA TN D-2040, 1964.

3. Pride, Richard A., Royster, Dick M., and Helms, Bobbie F.: Design, Tests, and Analysis of a Hot Structure for Lifting Reentry Vehicles. NASA TN D-2186, 1964.

4. Anon.: Comptes Rendus des Séances de la Onzième Conférence Générale des Poids et Mesures (Paris). Bur. Int. des Poids et Mesures, Oct. 11-20, 1960.

5. Chao, P. J., Payne, B. S., Jr., and Priest, D. K.: Development of a Cementation Coating Process for High-Temperature Protection of Molybdenum. ASD Tech. Rep. 61-241, U.S. Air Force, June 1961.

6. Stein, Bland A., and Lisagor, W. Barry: Diffusion Studies of Several Oxidation Resistant Coatings on Mo-0.5Ti Molybdenum Alloy at 2,500° F. NASA TN D-2039, 1964.

7. Anderson, Melvin S., and Stroud, C. W.: Experimental Observations of Aerodynamic and Heating Tests on Insulating Heat Shields. NASA TN D-1237, 1962.

8. Blumenthal, Herman, and Rothman, Neil: Development of a Powder and/or Gas Cementation Process for Coating Molybdenum Alloys for High Temperature Protection. Final Report (Contract No. AF 33(616)-7383), Wright Air Dev. Div., U.S. Air Force, July 1961.

9. Mathauser, Eldon E., Stein, Bland A., and Rummler, Donald R.: Investigation of Problems Associated With the Use of Alloyed Molybdenum Sheet in Structures at Elevated Temperatures. NASA TN D-447, 1960.

TABLE I.- THERMAL PROTECTION WEIGHTS OF THE HEAT-SHIELD PANELS

Component	Molybdenum alloy			Columbium alloy			Nickel alloy		
	Unit weight		Percent of total weight	Unit weight		Percent of total weight	Unit weight		Percent of total weight
	lb/ft^2	N/m^2		lb/ft^2	N/m^2		lb/ft^2	N/m^2	
Corrugated outer skins	0.587	28.11	53.2	0.564	27.00	57.9	0.396	18.96	48.0
Shield supports	.037	1.77	3.4	.041	1.96	4.3	.030	1.44	3.6
Rivets	.037	1.77	3.4				.030	1.44	3.6
Coating	.073	3.50	6.6						
Insulation	.160	7.66	14.5	.160	7.66	16.4	.160	7.66	19.4
Channels	.100	4.79	9.1	.100	4.79	10.3	.100	4.79	12.1
Rods	.109	5.22	9.9	.109	5.22	11.2	.109	5.22	13.2
Total weight	1.103	52.82		0.974	46.63		0.825	39.51	

TABLE II.- RESULTS OF ROOM-TEMPERATURE TENSILE TESTS OF AS-RECEIVED MOLYBDENUM-ALLOY SHEET IN STRESS-RELIEVED CONDITION

[Nominal strain rate: 0.005 per minute (0.000083 per second) to yield, 0.050 per minute (0.00083 per second) to failure]

Grain direction	Ultimate stress		0.2-percent-offset yield stress		Young's modulus		Elongation in 2-inch (5.1-cm) gage length, percent
	ksi	MN/m^2	ksi	MN/m^2	psi	GN/m^2	
Longitudinal	129.0	889.5	109.3	753.6	39.0×10^6	268.9	7.5
	133.1	917.7	112.0	772.2	40.0	275.8	11.7
	131.8	908.8	109.7	756.4	40.0	275.8	10.5
Transverse	134.7	928.8	125.6	866.0	39.5×10^6	272.4	3.5
	136.3	939.8	123.2	849.5	40.5	279.2	5.5
	134.7	928.8	122.8	846.7	38.5	265.5	4.5

TABLE III.- RESULTS OF TENSILE TESTS ON MOLYBDENUM-ALLOY SHEET COATED WITH SILICIDE-BASE COATING

[Nominal strain rate: 0.005 per minute (0.000083 per second) to yield, 0.050 per minute (0.00083 per second) to failure]

Temperature (a)		Ultimate stress (b)		0.2-percent-offset yield stress (b)		Young's modulus (b)		Elongation in 2-inch (5.1-cm) gage length, percent
°F	°K	ksi	MN/m^2	ksi	MN/m^2	psi	GN/m^2	
75	297	97.4	671.6	65.7	453.0	42.5×10^6	293.0	8
75	297	96.8	667.4	69.6	479.9	41.7	287.5	8
75	297	93.2	642.6	64.1	442.0	44.6	307.5	8
75	297	92.3	636.4	64.6	445.4	42.4	292.3	8
1,938	1,332	44.8	308.9	42.7	294.4	33.9	233.7	2
2,435	1,608	13.9	95.8	13.0	89.6	20.1	138.6	3
2,908	1,871	14.5	100.0	7.1	49.0	8.5	58.6	15
[c]2,400	1,589	17.0	117.2	16.6	114.5	19.4	133.8	2

[a]Optical pyrometer at 0.65μ, based on 0.8 emissivity.
[b]Stress based on area before coating.
[c]After 5 hours exposure in air at 2,400° F (1,589° K).

TABLE IV.- RESULTS OF ROOM-TEMPERATURE TENSILE TESTS OF AS-RECEIVED COLUMBIUM-ALLOY SHEET IN ANNEALED CONDITION

[Nominal strain rate: 0.005 per minute (0.000083 per second) to yield, 0.050 per minute (0.00083 per second) to failure]

Grain direction	Ultimate stress		0.2-percent-offset yield stress		Young's modulus		Elongation in 2-inch (5.1-cm) gage length, percent
	ksi	MN/m^2	ksi	MN/m^2	psi	GN/m^2	
Longitudinal	74.6	514.4	56.0	386.1	17.2×10^6	118.6	20
	75.8	522.6	57.4	395.8	17.8	122.7	20
	78.5	541.3	62.0	427.5	17.5	120.7	19
	78.4	540.6	62.5	430.9	17.3	119.3	18
Transverse	76.9	530.2	58.0	399.9	16.9×10^6	116.5	18
	75.4	519.9	56.8	391.6	17.1	117.9	18
	76.8	529.5	57.0	393.0	17.0	117.2	18
	76.1	524.7	56.6	390.3	17.4	120.0	18

TABLE V.- RESULTS OF OXIDATION TESTS ON MOLYBDENUM-ALLOY COUPONS

COATED WITH SILICIDE-BASE COATING

Type of coupon	Type of test	Test temperature		Time to failure	
		°F	°K	hours	ks
Single coated	Continuous	2,700	1,755	15.5	55.8
		2,700	1,755	22.3	80.3
		2,500	1,644	34.0	122.4
		2,500	1,644	36.2	130.3
		2,500	1,644	38.2	137.5
		2,500	1,644	39.3	141.5
		2,500	1,644	41.6	149.8
		2,500	1,644	42.4	152.6
		2,000	1,366	10.5	37.8
		2,000	1,366	>672	>2,419
		2,000	1,366	>1,010	>3,636
		1,700	1,200	>250	>900
		1,450	1,061	>250	>900
	1.0-hr cyclic	2,900	1,866	14.0	50.4
		2,700	1,755	23.5	84.6
		2,500	1,644	[a]2.4	[a]8.6
		2,500	1,644	24.5	88.2
		2,500	1,644	53.4	192.2
		2,200	1,478	45.5	163.8
		2,000	1,366	69.5	250.2
	0.5-1.0-0.5-hr cyclic	2,500	1,644	7.9	28.4
		2,500	1,644	3.4	12.2
		2,500	1,644	7.5	27.0
	0.1-hr cyclic	2,500	1,644	1.2	4.3
		2,500	1,644	.7	2.5
		2,500	1,644	6.0	21.6
Double coated	Continuous	2,500	1,644	61.9	222.8
		2,500	1,644	60.2	216.7
	1.0-hr cyclic	2,700	1,755	21.0	75.6
		2,500	1,644	15.5	55.8
		2,500	1,644	54.5	196.2
		2,500	1,644	73.4	264.2
		2,000	1,366	94.0	338.4
	0.1-hr cyclic	2,500	1,644	26.2	94.3
		2,500	1,644	34.5	124.2

[a]An imperfection in the coating was noted before testing and failure occurred at the imperfection.

TABLE VI.- RESULTS OF OXIDATION TESTS ON MOLYBDENUM-ALLOY RIVETED CONFIGURATIONS COATED WITH SILICIDE-BASE COATING UNDER 1.0-HOUR CYCLIC CONDITIONS

Specimen configuration	Coating application	Test temperature		Time to failure	
		°F	°K	hours	ks
Sheet V	Single coated	2,900	1,866	7.9	28.4
		2,700	1,755	14.2	51.1
		2,400	1,589	60.0	216.0
		2,000	1,366	52.5	189.0
	Double coated	2,900	1,866	3.8	13.7
		2,700	1,755	5.8	20.9
		2,400	1,589	35.9	129.2
		2,000	1,366	16.9	60.8
Sheet Z	Single coated	2,900	1,866	15.0	54.0
		2,800	1,811	4.1	14.8
		2,500	1,644	12.5	45.0
		2,500	1,644	20.0	72.0
		2,200	1,478	37.0	133.2
		2,000	1,366	65.5	235.8
	Double coated	2,000	1,366	9.5	34.2

TABLE VII.- EFFECT OF EXPOSURE TIME AND TEMPERATURE ON SUBSTRATE THICKNESS FOR MOLYBDENUM-ALLOY SHEET COATED WITH SILICIDE-BASE COATING

Specimen	Type of test	Test temperature		Exposure time		Substrate thickness			
						As coated		After test	
		°F	°K	hours	ks	inches	μm	inches	μm
Coupon	Continuous	2,000	1,366	1	3.6	0.0100	254.0	0.0099	251.5
	Continuous			20	72.0	.0100	254.0	.0097	246.4
	1.0-hr cyclic			70	252.0	.0100	254.0	.0099	251.5
	Continuous			672	2,419	.0100	254.0	.0088	223.5
	Continuous			1,010	3,636	.0100	254.0	.0084	213.4
Sheet V	1.0-hr cyclic			17	61.2	0.0092	233.7	0.0090	228.6
	1.0-hr cyclic			53	190.8	.0095	241.3	.0093	236.2
Sheet Z	1.0-hr cyclic			65	234.0	0.0100	254.0	0.0097	246.4
Sheet V	1.0-hr cyclic	2,400	1,589	36	129.6	0.0092	233.7	0.0077	195.6
	1.0-hr cyclic			60	216.0	.0095	241.3	.0078	198.1
Coupon	Continuous	2,500	1,644	1	3.6	0.0093	236.2	0.0081	205.7
	Continuous			8	28.8	.0093	236.2	.0074	188.0
	Continuous			47	169.2	.0093	236.2	.0068	172.7
Coupon	Continuous	2,700	1,755	1	3.6	0.0100	254.0	0.0082	208.3
	Continuous			5	18.0	.0100	254.0	.0072	182.9
	Continuous			26	93.6	.0100	254.0	.0066	167.6
	1.0-hr cyclic			21	75.6	.0092	233.7	.0058	147.3
	1.0-hr cyclic			23	82.8	.0100	254.0	.0062	157.5
Sheet V	1.0-hr cyclic			6	21.6	0.0092	233.7	0.0066	167.6
	1.0-hr cyclic			14	50.4	.0095	241.3	.0069	175.3
Coupon	1.0-hr cyclic	2,900	1,866	1	3.6	0.0093	236.2	0.0066	167.6
	1.0-hr cyclic			14	50.4	.0093	236.2	.0055	139.7
Sheet V	1.0-hr cyclic			8	28.8	0.0095	241.3	0.0067	170.2

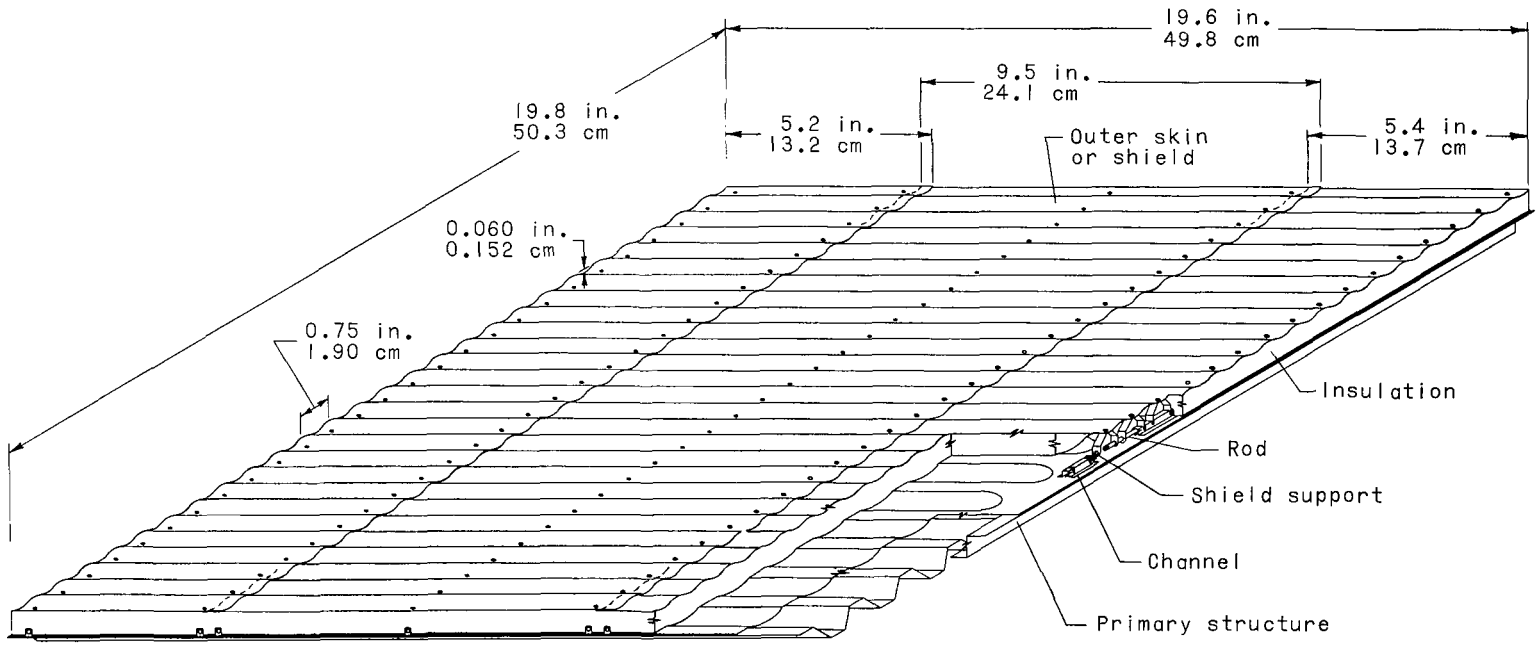

(a) Panel assembly.

Figure 1.- Design details of heat-shield panels.

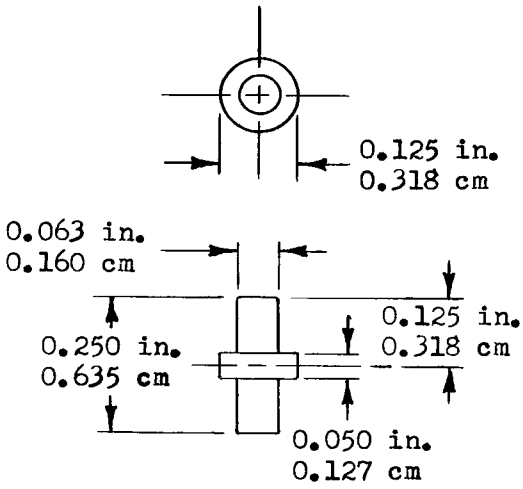

(b) Rivet design for nickel-alloy and molybdenum-alloy shields.

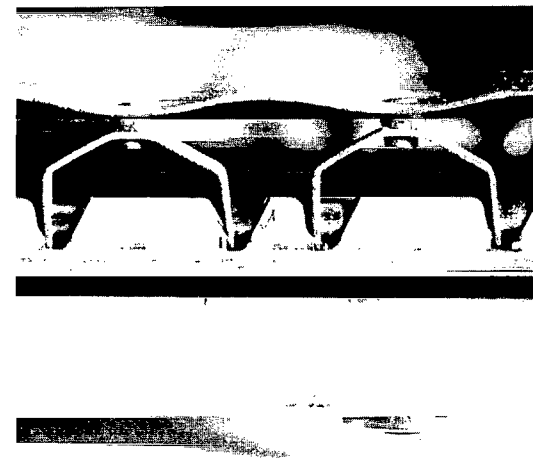

(c) Riveted joints on molybdenum-alloy shields after application of silicide-base coating.

(d) Spot-welded joints on columbium-alloy shields.

Figure 1.- Concluded. L-64-4723

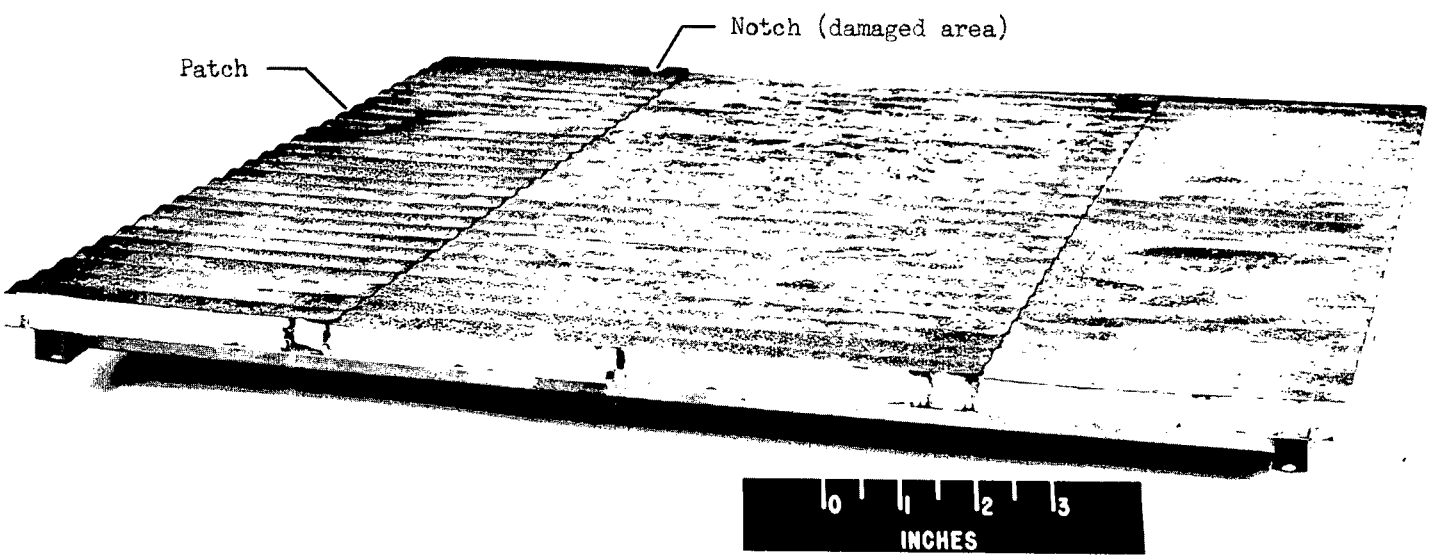

Figure 2.- Molybdenum-alloy panel after assembly. L-63-1322.1

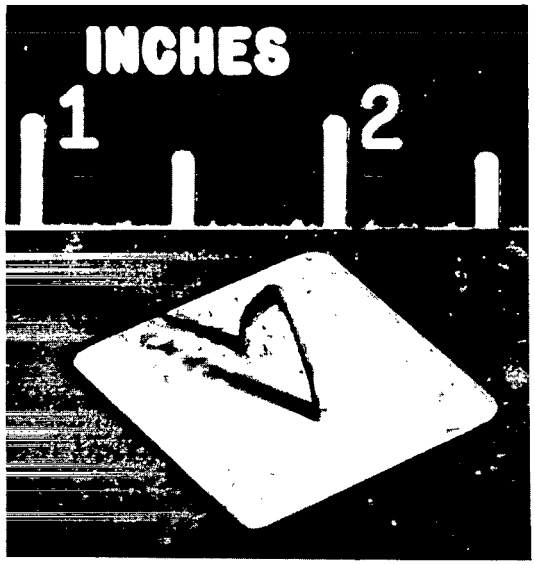

Single coated

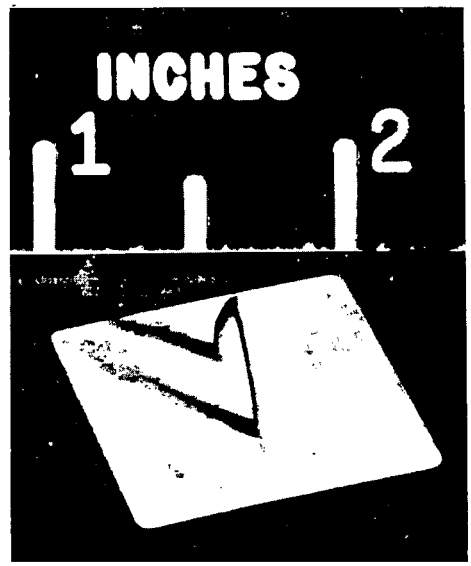

Double coated

(a) Sheet-V configuration.

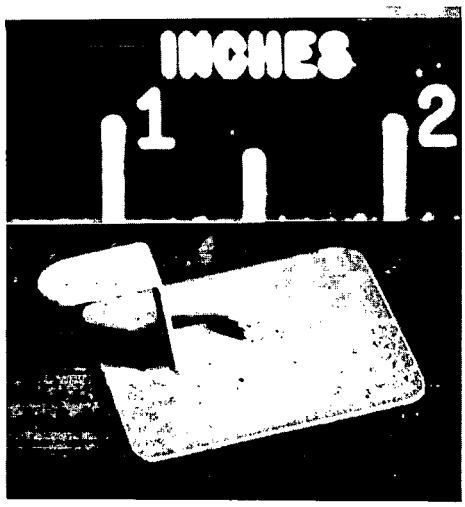

Single coated

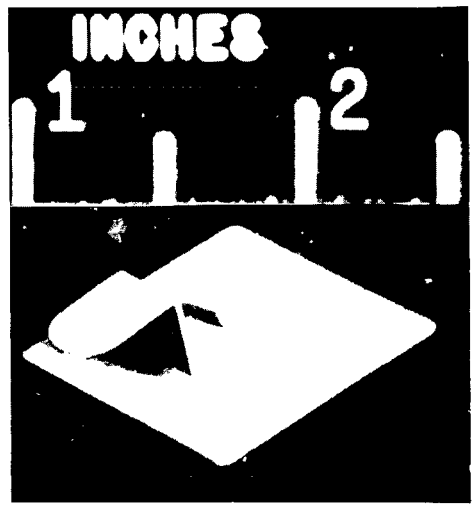

Double coated

(b) Sheet-Z configuration. L-64-4724

Figure 3.- Appearance of as-coated molybdenum-alloy riveted specimens.

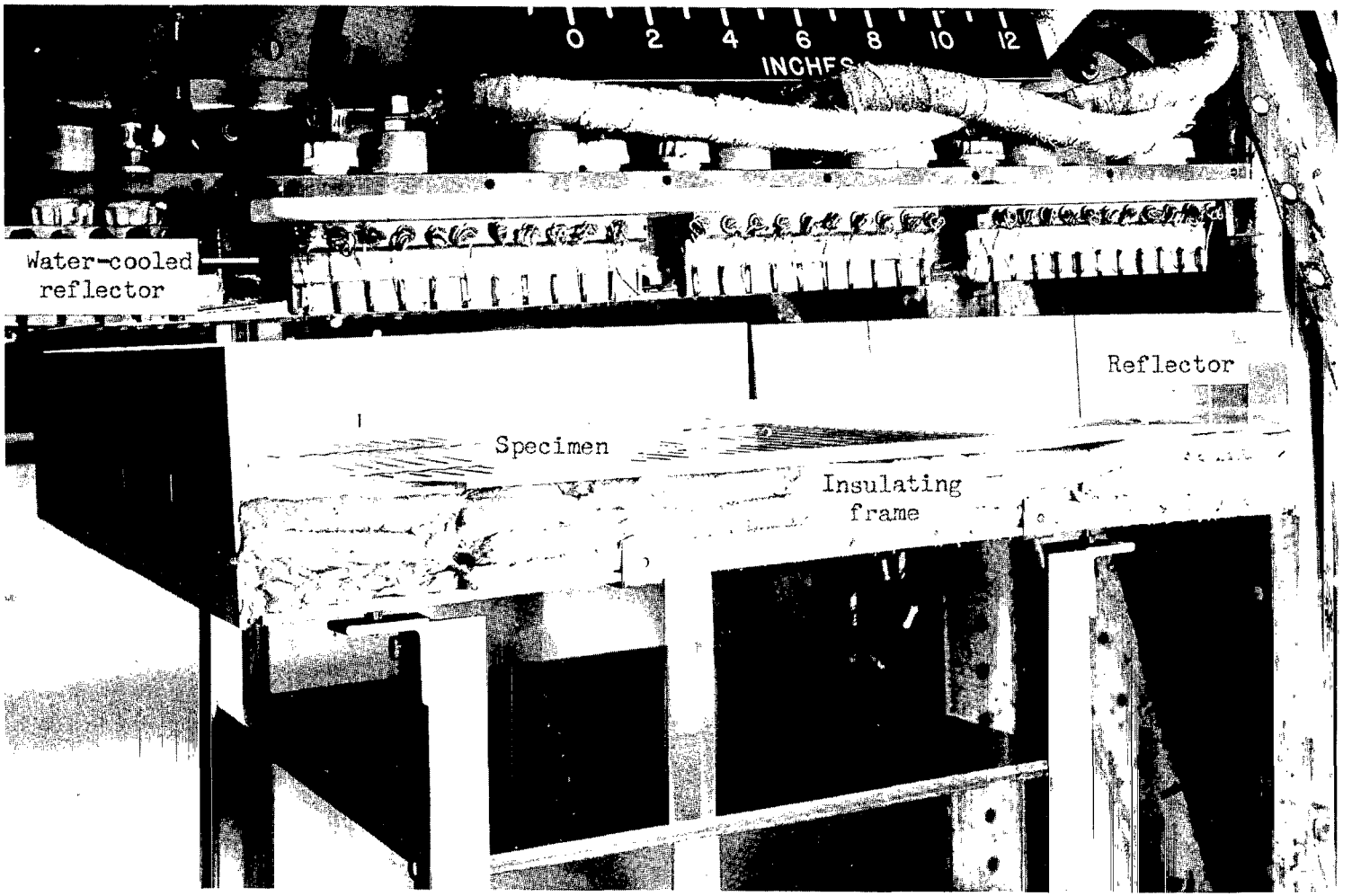

Figure 4.- Radiant-heating test setup. L-61-4397.1

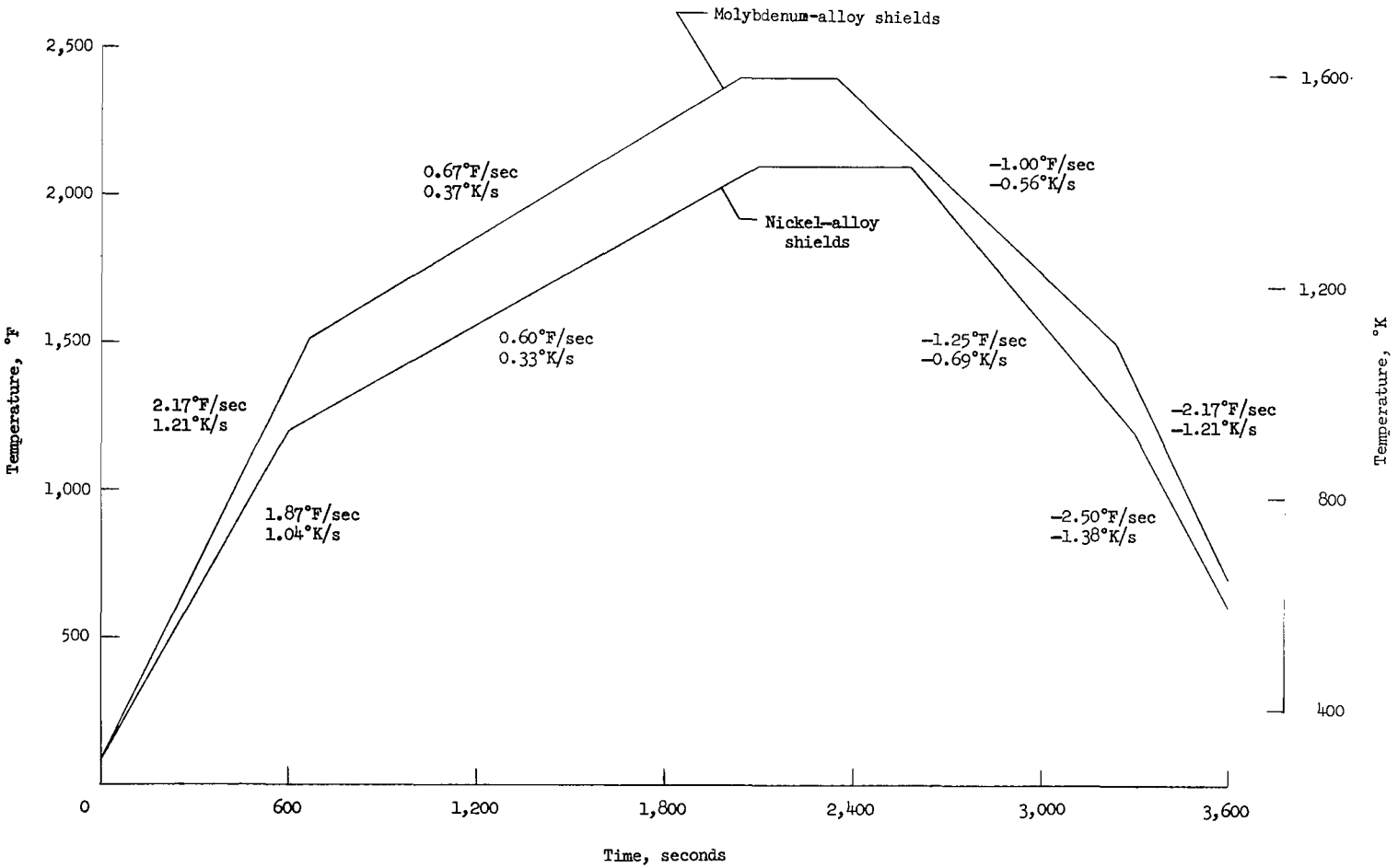

Figure 5.- Programed temperature-time histories for nickel-alloy and molybdenum-alloy panels.

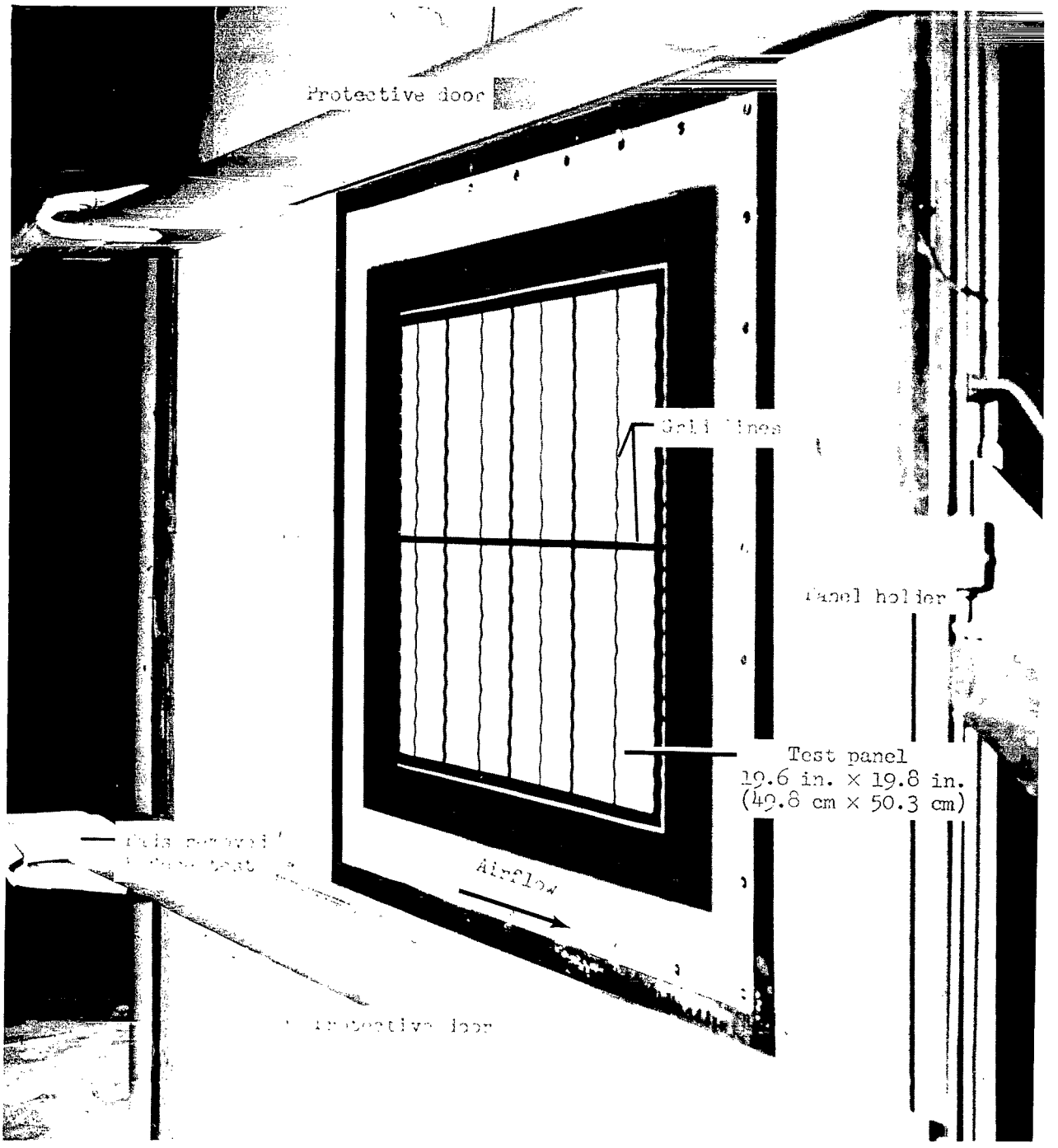

(a) Test panel mounted. L-63-3261.1

Figure 6.- Panel holder with protective doors in Langley 9- by 6-foot thermal structures tunnel.

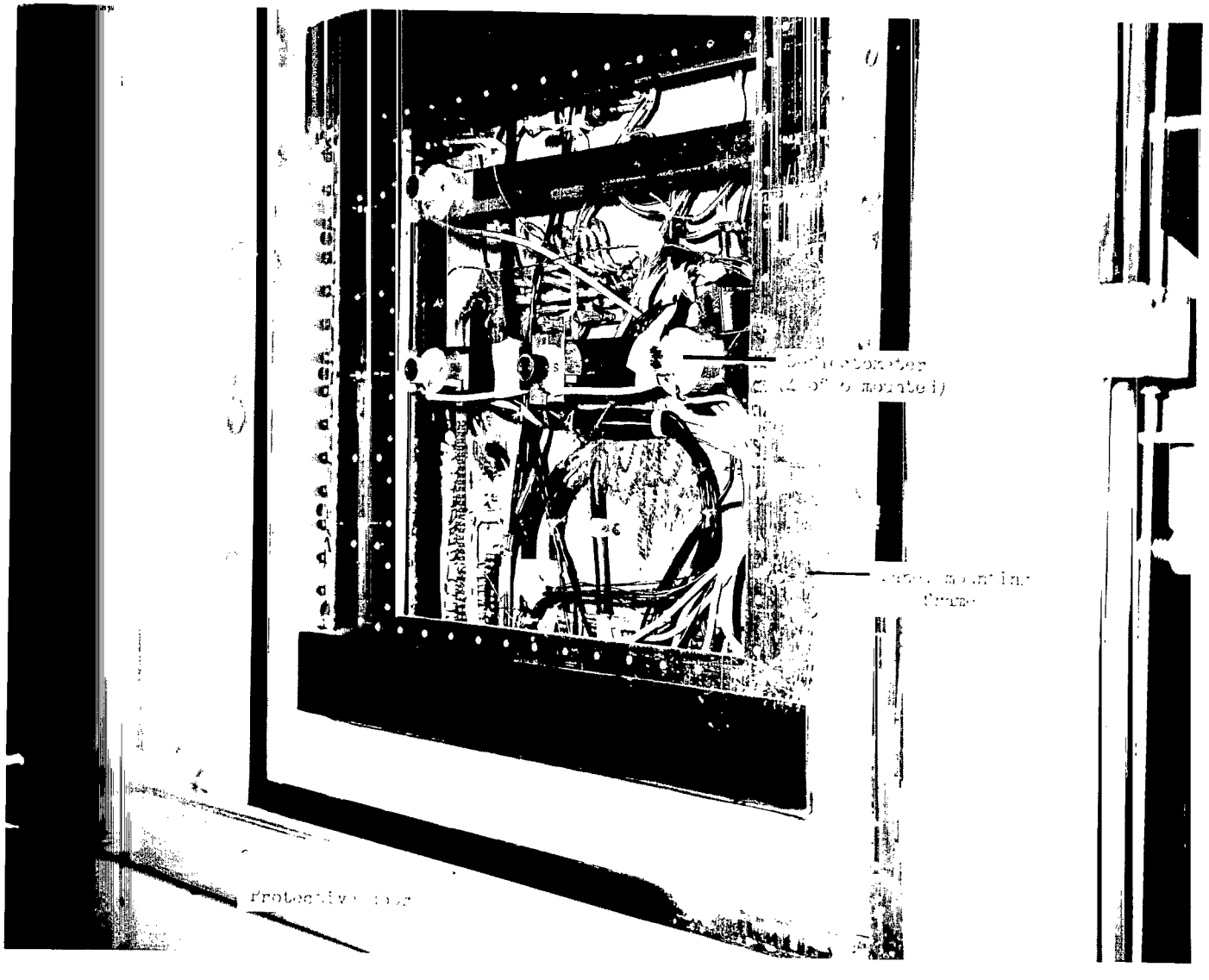

(b) Test panel removed.

L-63-3629.1

Figure 6.- Concluded.

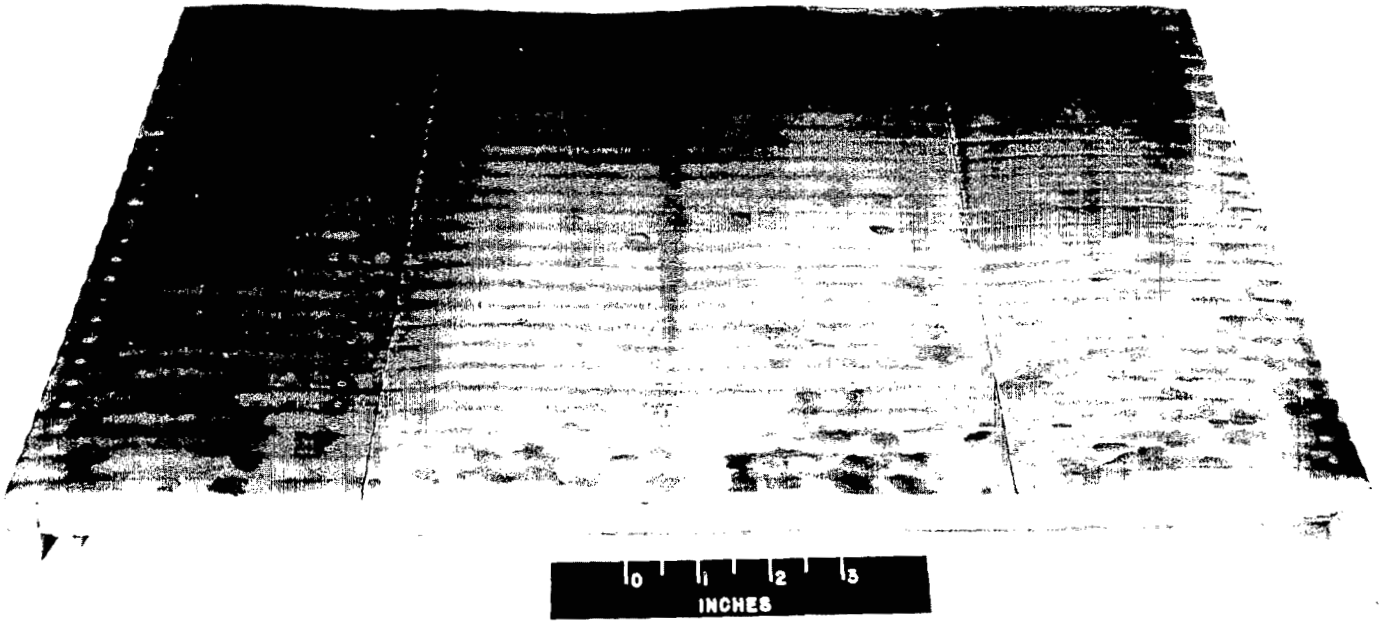

Figure 7.- Nickel-alloy panel after one radiant-heating cycle.

L-62-9678

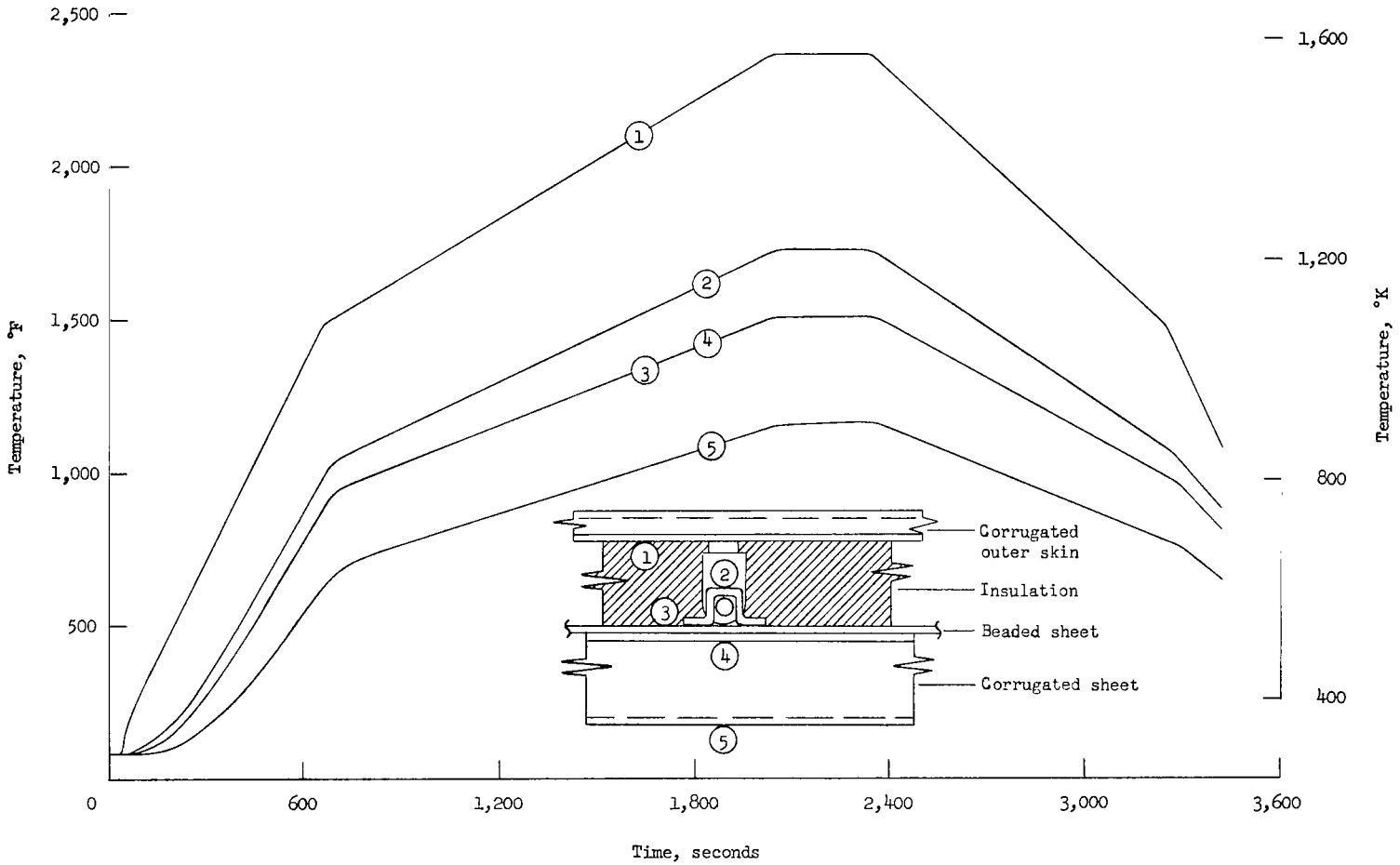

Figure 8.- Temperature distribution through molybdenum-alloy panel. Circled numbers indicate thermocouple locations.

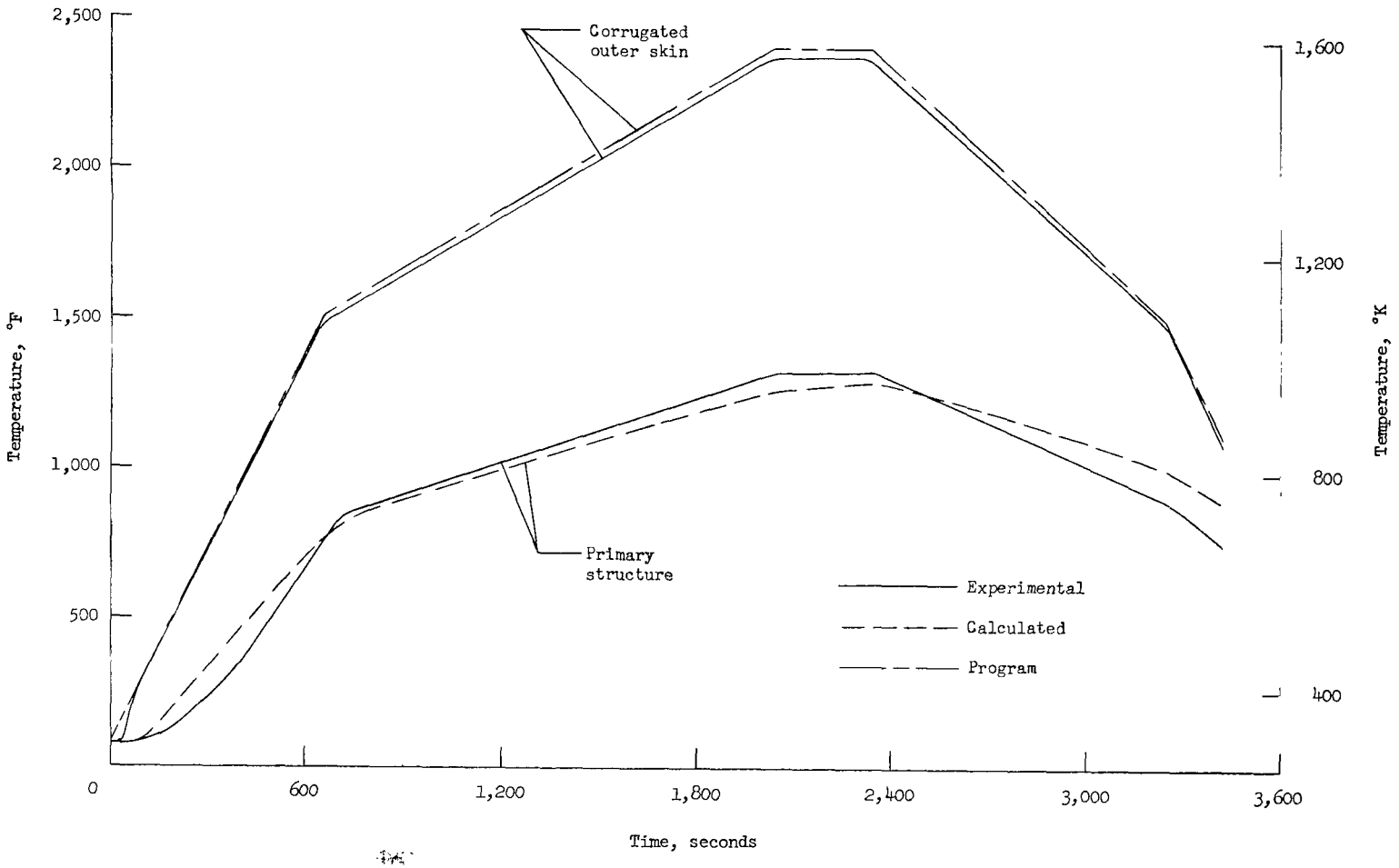

Figure 9.- Theoretical and measured temperatures for molybdenum-alloy panel.

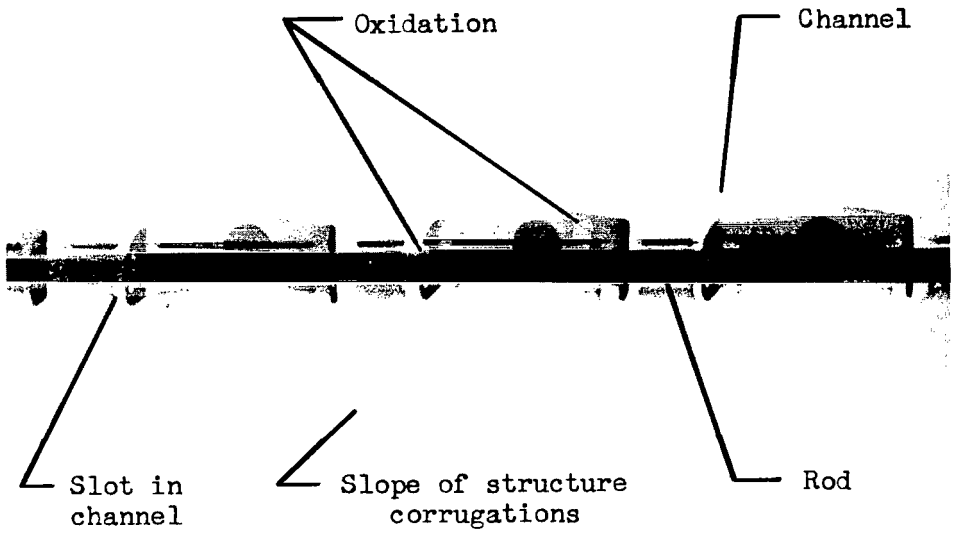

(a) Taken directly above panel.

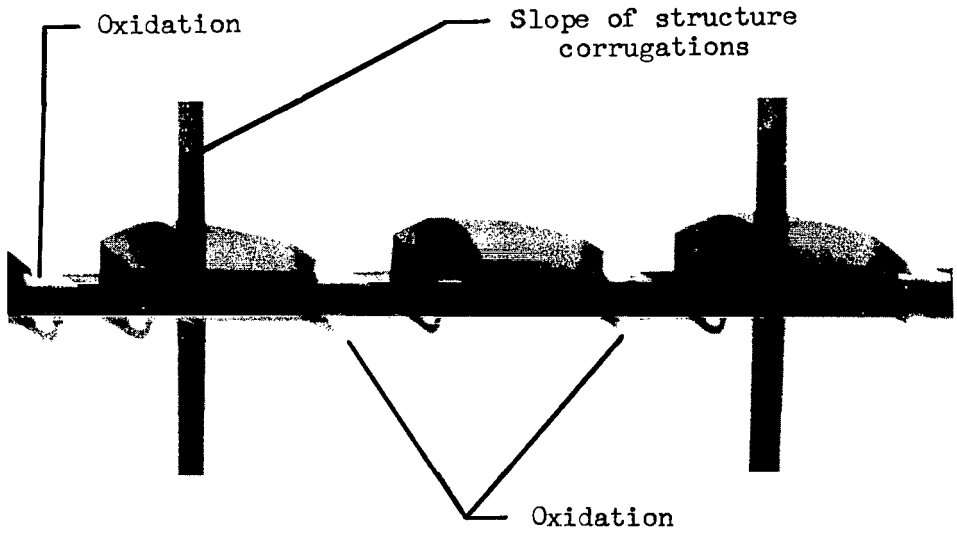

(b) Taken at an angle to panel. L-64-4725

Figure 10.- Radiographs showing deterioration of coated molybdenum-alloy panel.

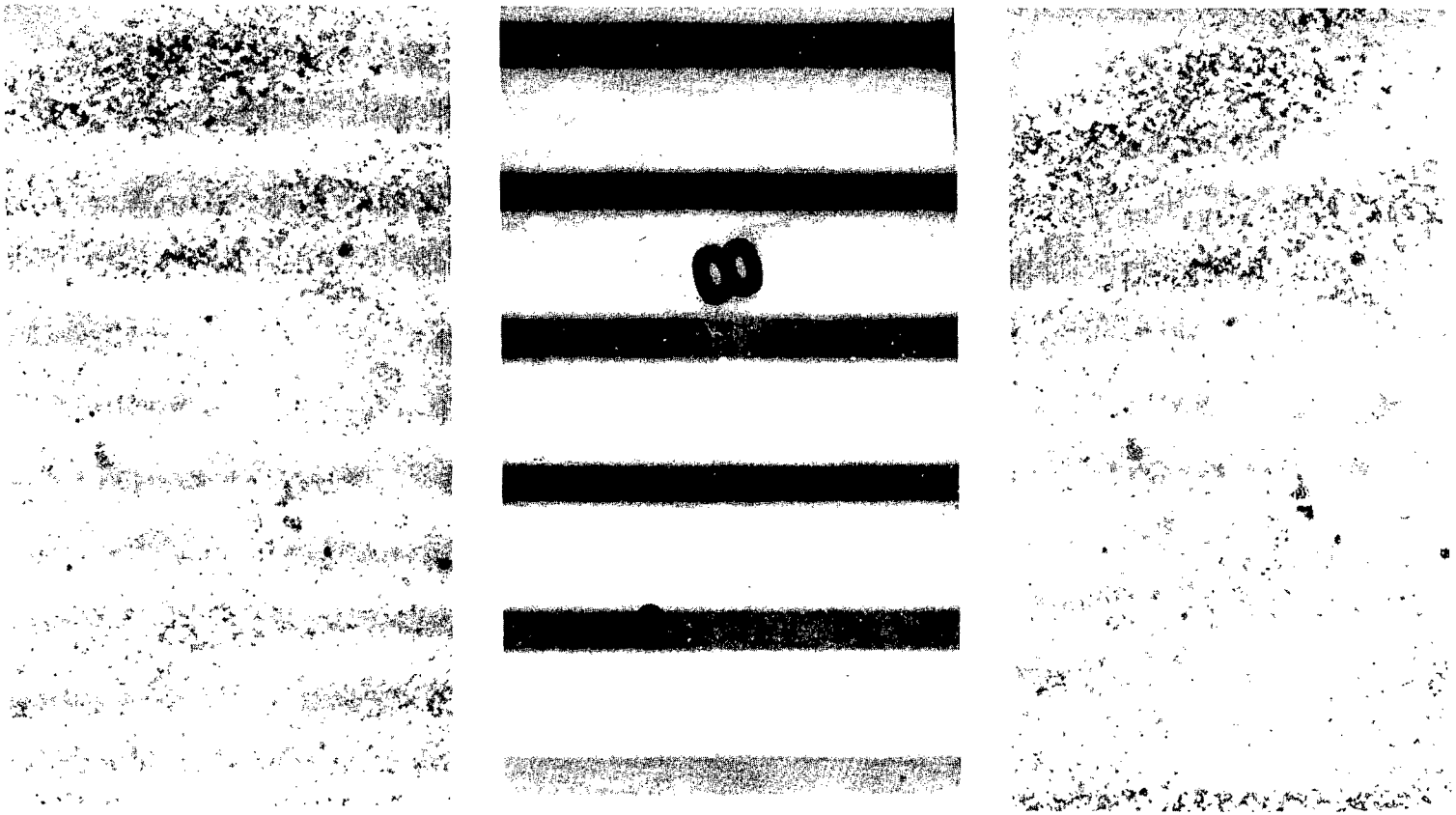

L-64-4726

(a) Photograph showing no visible damage.

(b) Radiograph indicating oxidation damage.

(c) Photograph showing holes in shield with coating removed.

Figure 11.- Radiographic detection of oxidation damage to coated molybdenum-alloy shield after five heating cycles.

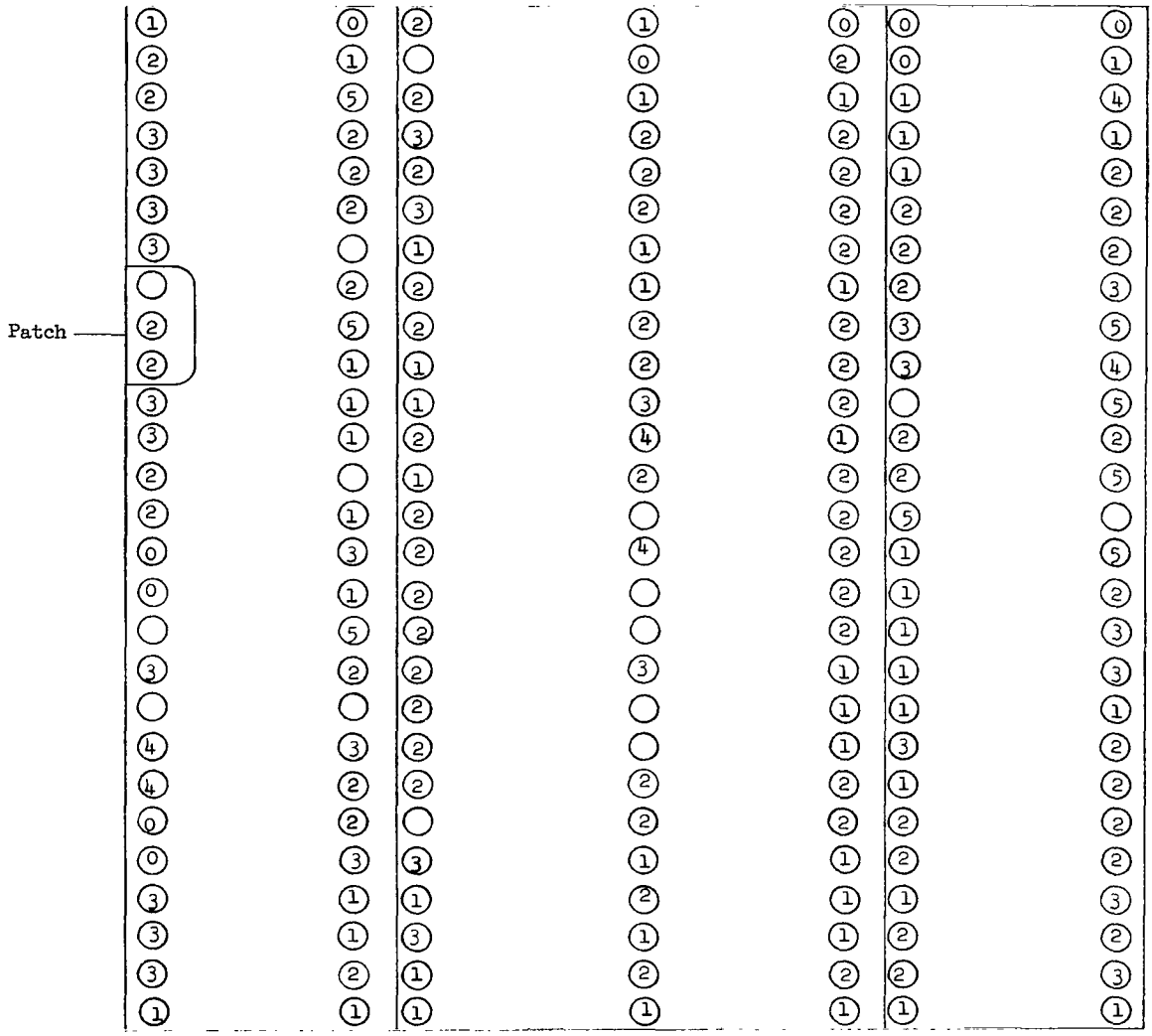

Cycle	Shield supports damaged, percent
0	5
1	31
2	70
3	85
4	88
5	92

Circles denote shield supports.

Numbers denote cycle in which first indication of mechanical or oxidation damage was noted.

Figure 12.- Location and percent of shield supports damaged for molybdenum-alloy panel.

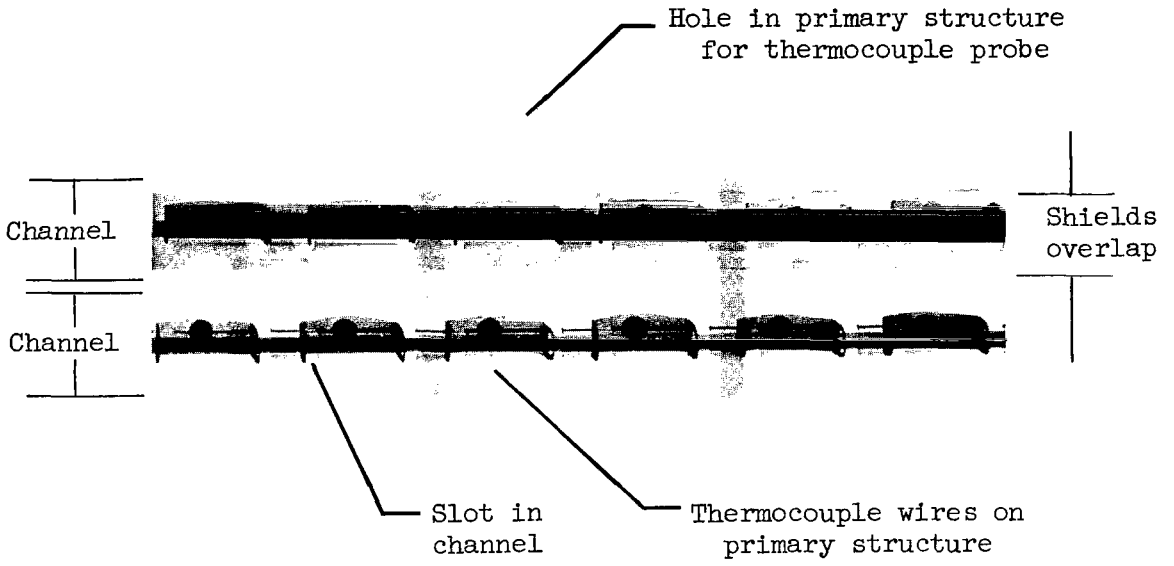

(a) Before heating tests.

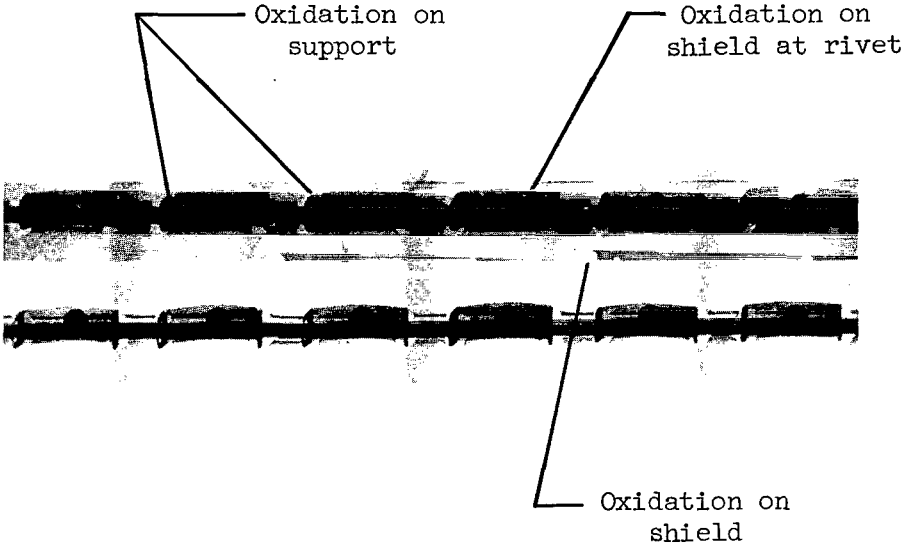

(b) After one heating cycle. L-64-4727

Figure 13.- Radiographs showing progressive deterioration of coated molybdenum-alloy panel.

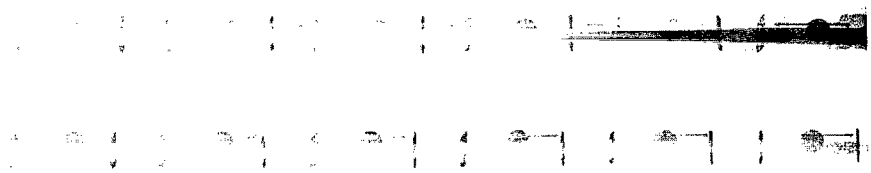

(c) After two heating cycles.

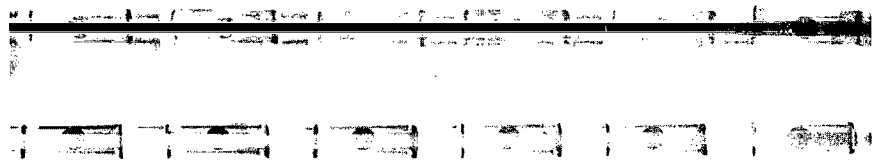

(d) After five heating cycles. L-64-4728

Figure 13.- Concluded.

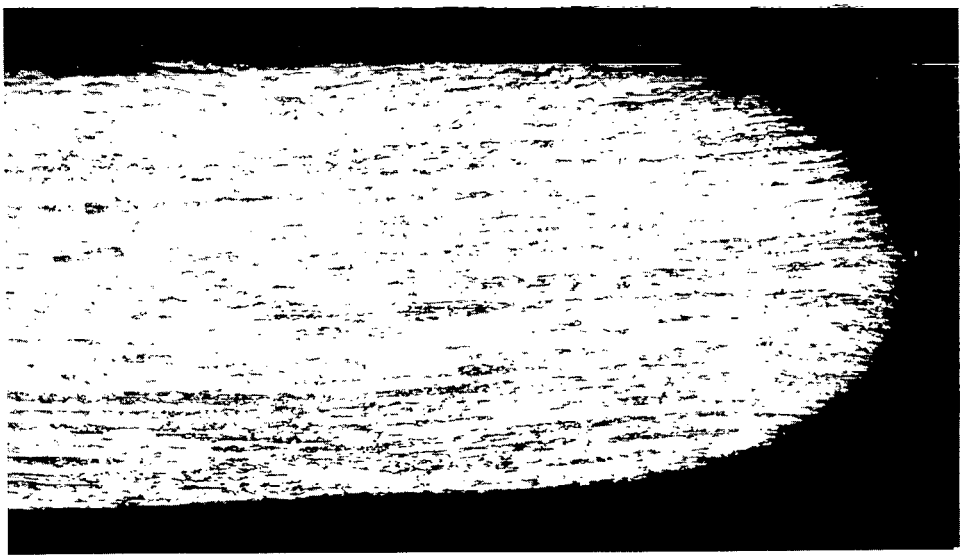

(a) Before coating.

(b) As coated. L-64-4729

Figure 14.- Typical cross-sectional views of molybdenum-alloy sheet before and after coating. ×200.

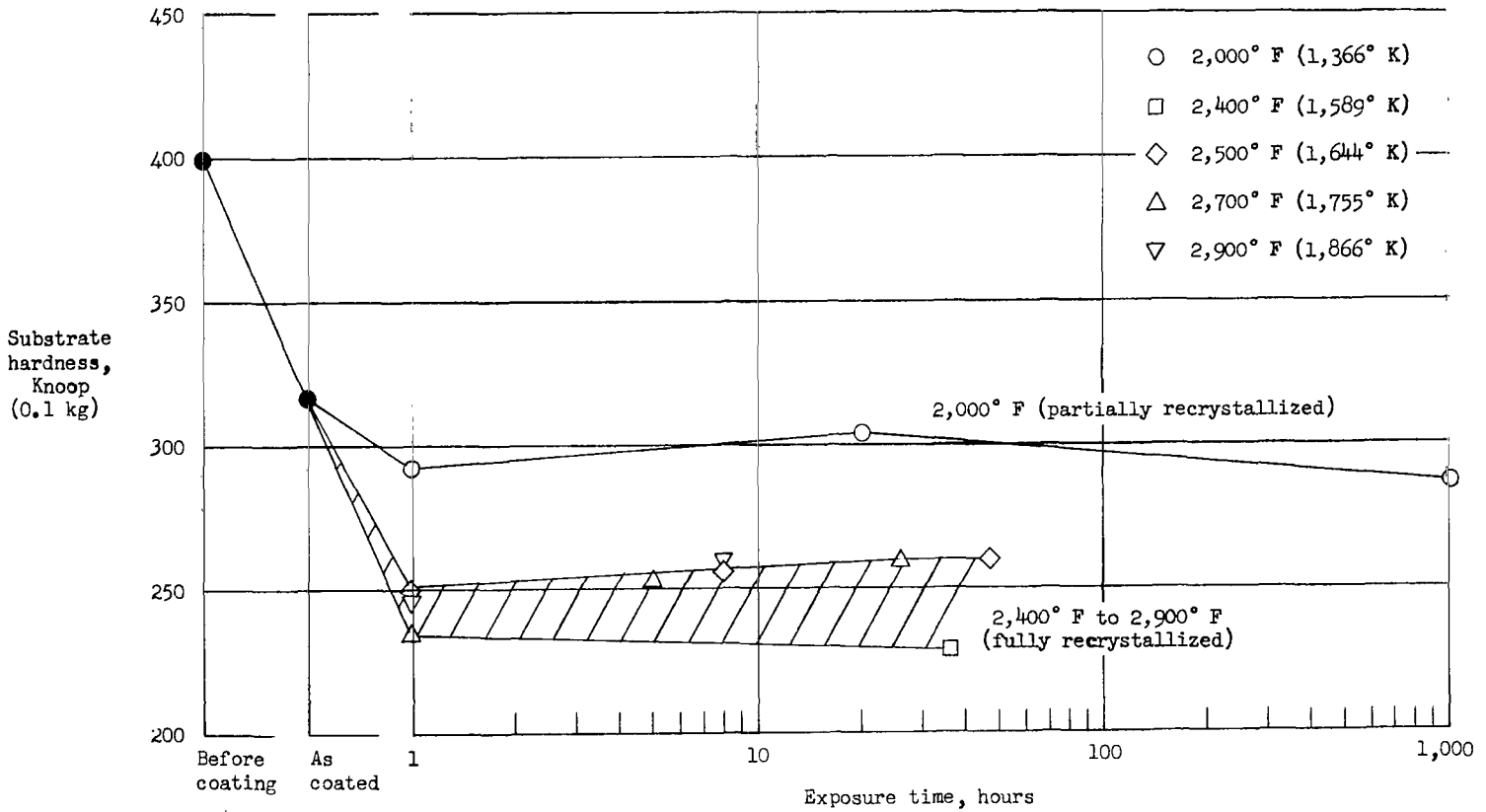

Figure 15.- Variation of substrate hardness with exposure time and temperature for molybdenum-alloy sheet coated with silicide-base coating.

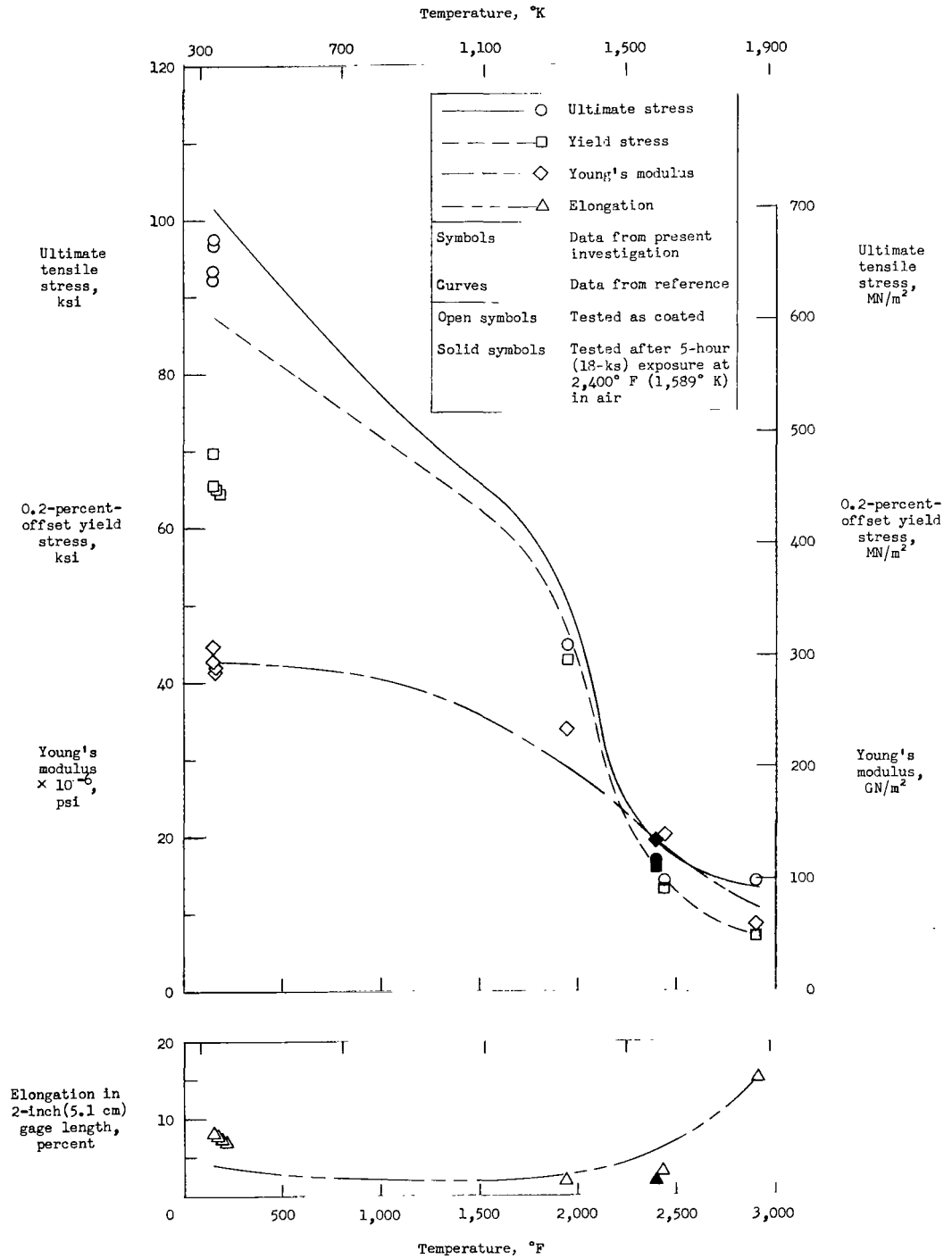

Figure 16.- Tensile test results for coated molybdenum-alloy sheet at various temperatures determined in present investigation compared with previous tensile data reported for coated molybdenum-alloy sheet in reference 9.

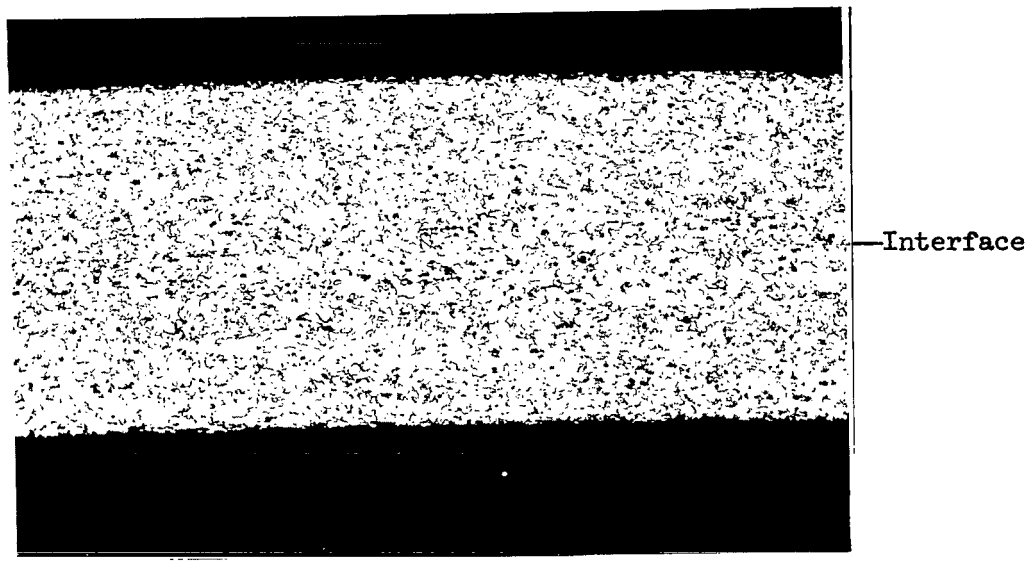

(a) ×100.

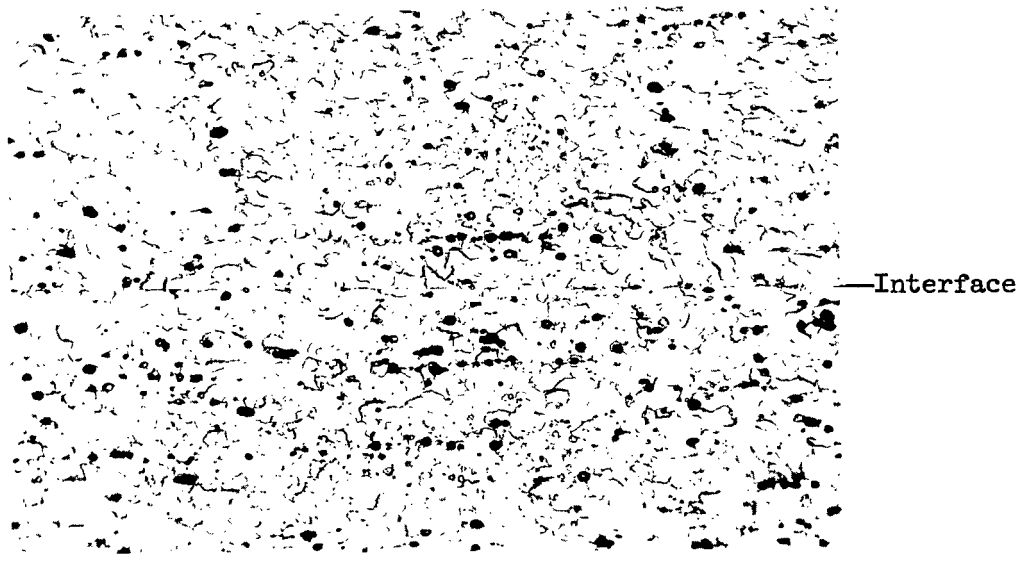

(b) ×250. L-64-4730

Figure 17.- Cross-sectional views of spot weld in 0.010-in. (0.254-mm) columbium-alloy sheets.

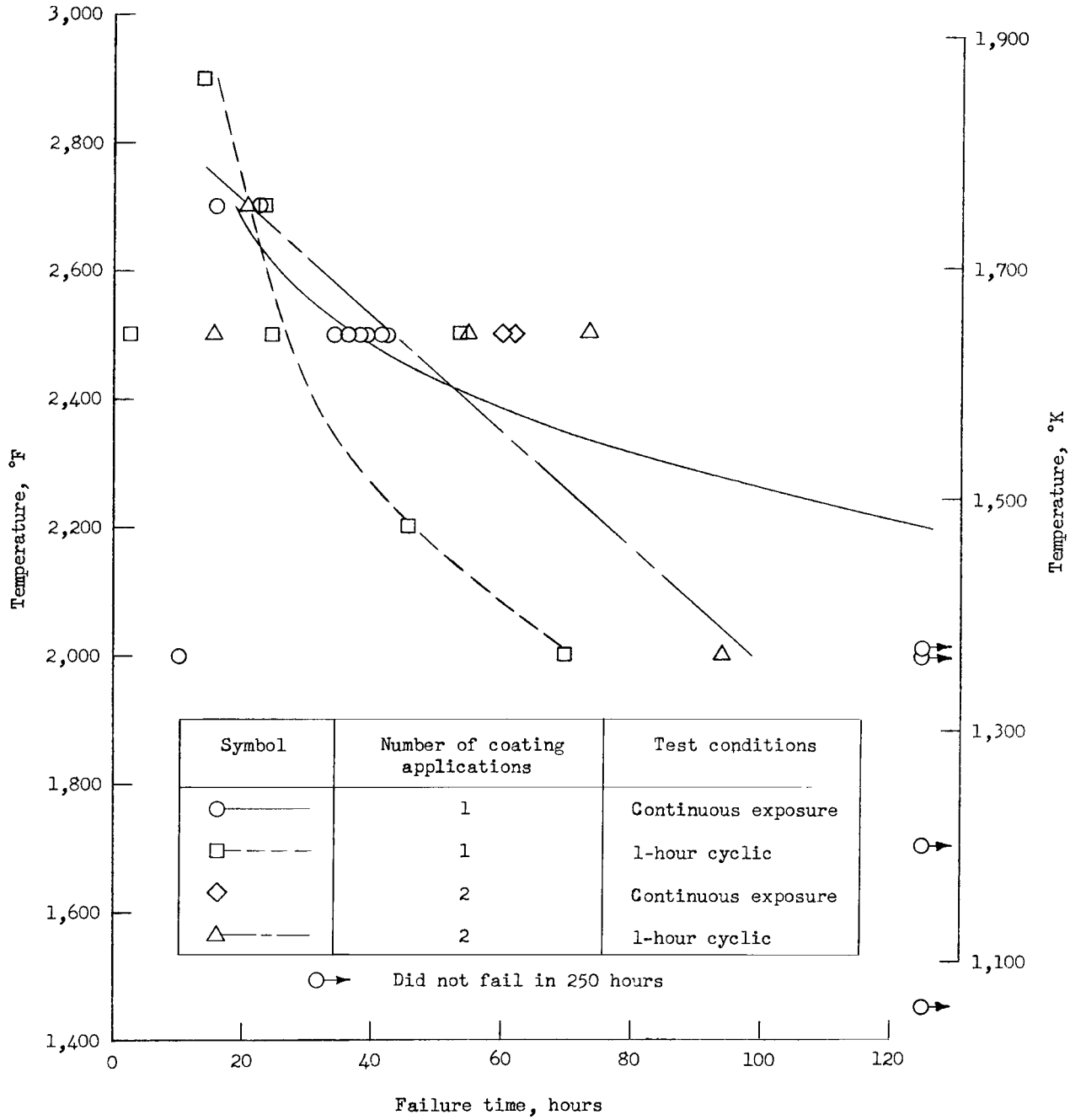

Figure 18.- Continuous and cyclic exposure life for silicide-base coating on molybdenum-alloy sheet coupons at various temperatures.

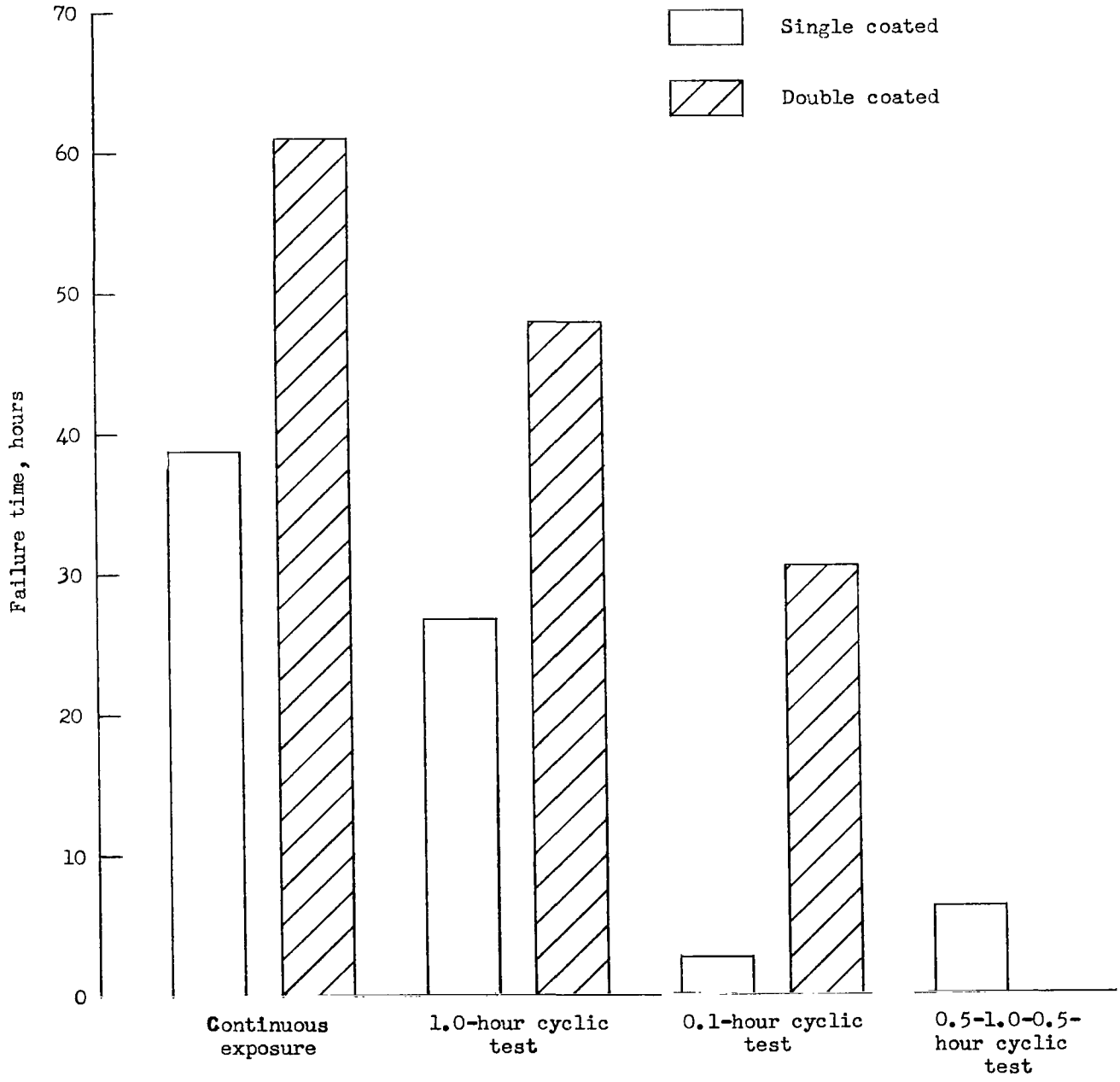

Figure 19.- Effect of various test conditions on coating life of coated molybdenum-alloy coupons at 2,500° F (1,644° K).

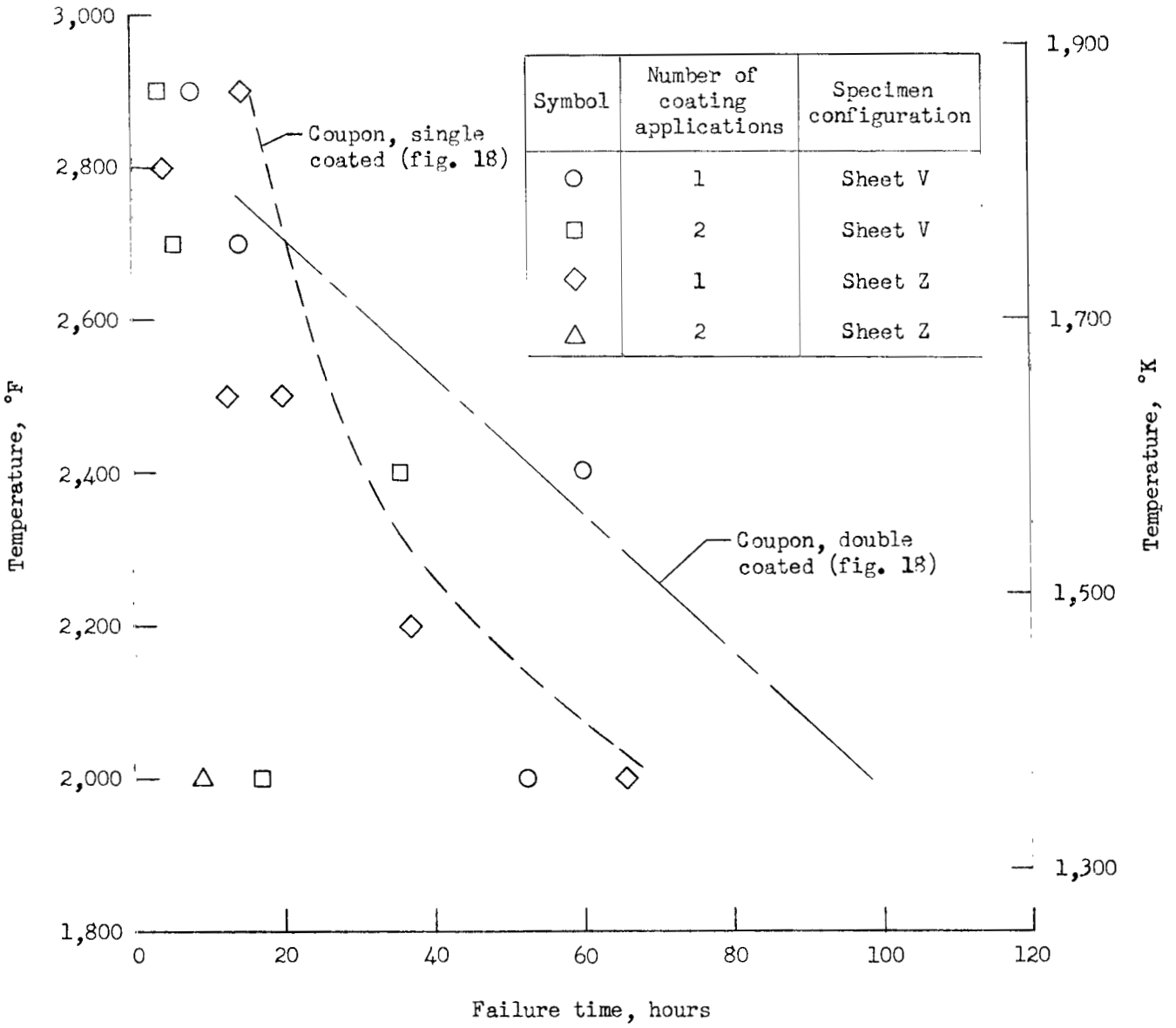

Figure 20.- Comparison of coating life on small riveted molybdenum-alloy specimens (symbols) with that on sheet coupons (curves) at various temperatures under 1.0-hour cyclic conditions.

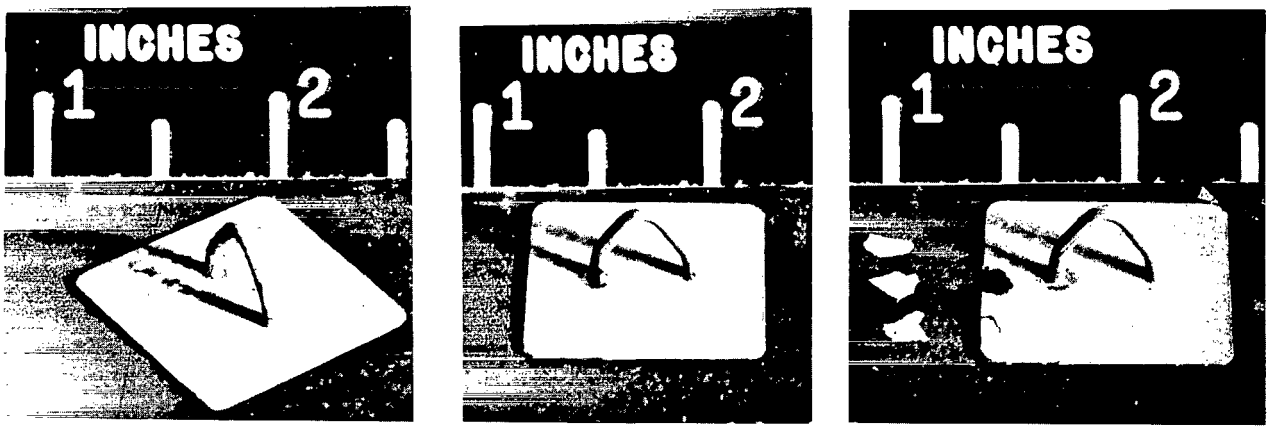

As coated | After 5 cycles | After 14 cycles

(a) Single coated.

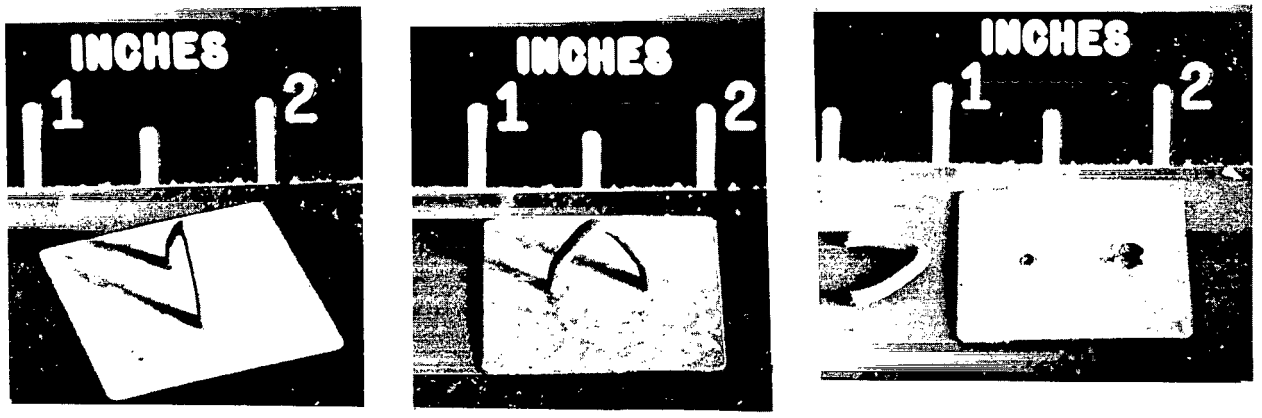

As coated | After 5 cycles | After 6 cycles

(b) Double coated.

L-64-4731

Figure 21.- Molybdenum-alloy sheet-V specimens coated with silicide-base coating before and after 1.0-hour cyclic tests at 2,700° F (1,755° K).

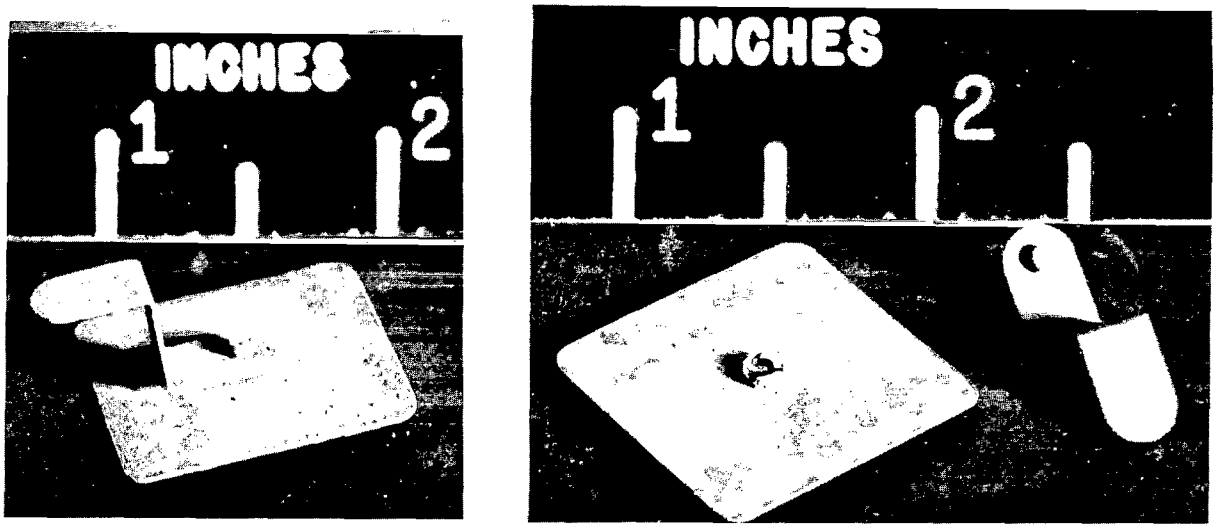

As coated

After 68 cycles

(a) Single coated.

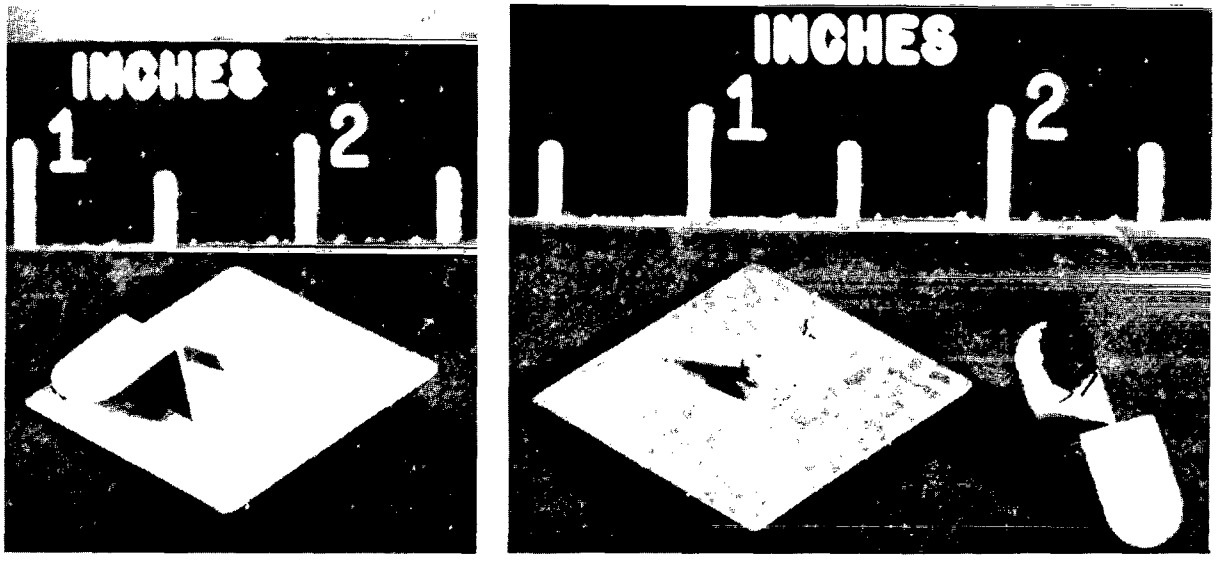

As coated

After 9 cycles

(b) Double coated.

L-64-4732

Figure 22.- Molybdenum-alloy sheet-Z specimens coated with silicide-base coating before and after 1.0-hour cyclic tests at 2,000° F (1,366° K).

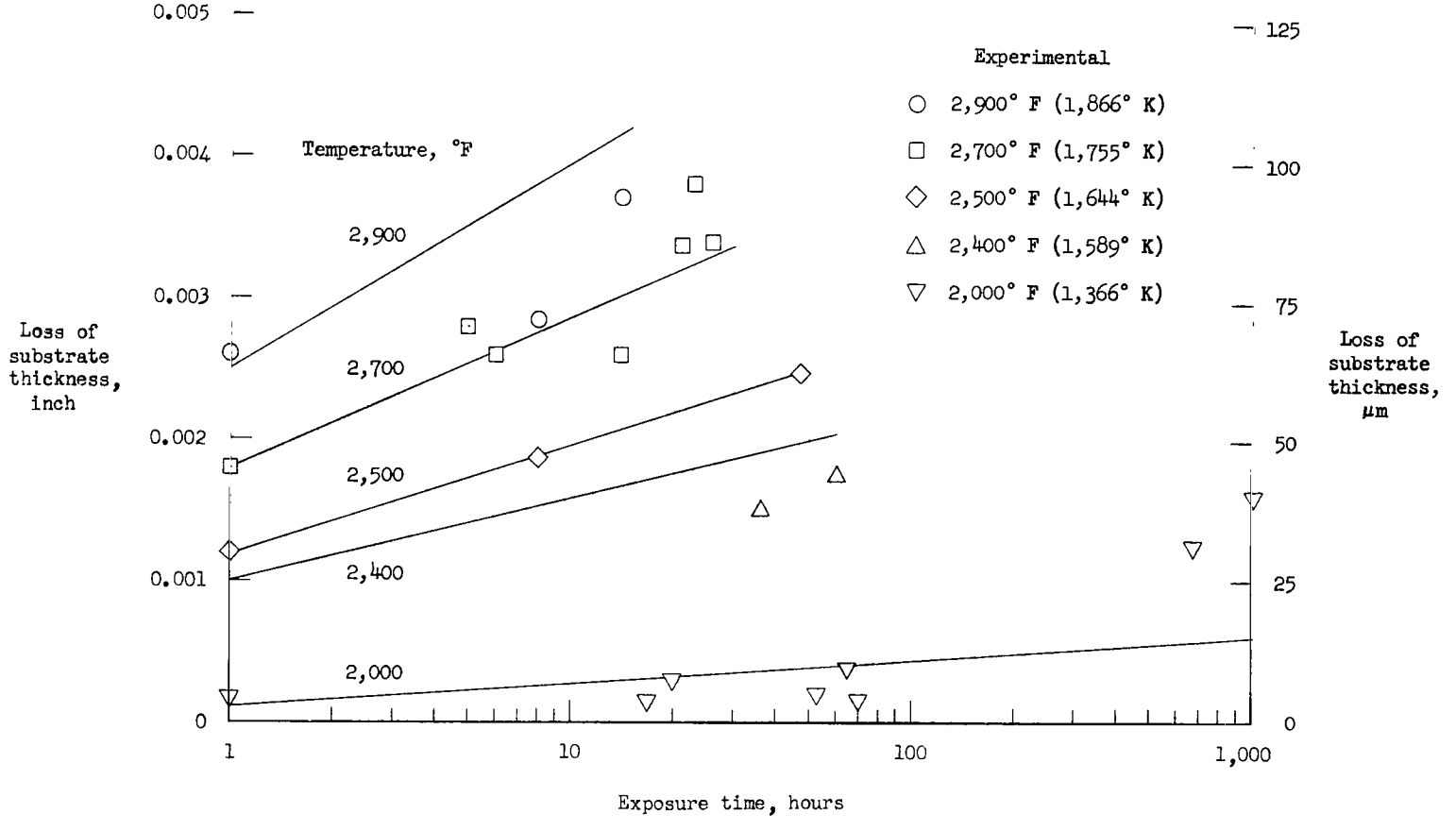

Figure 23.- Loss of substrate thickness due to diffusion of silicide-base coating into molybdenum-alloy substrate for various time-temperature exposures in air.

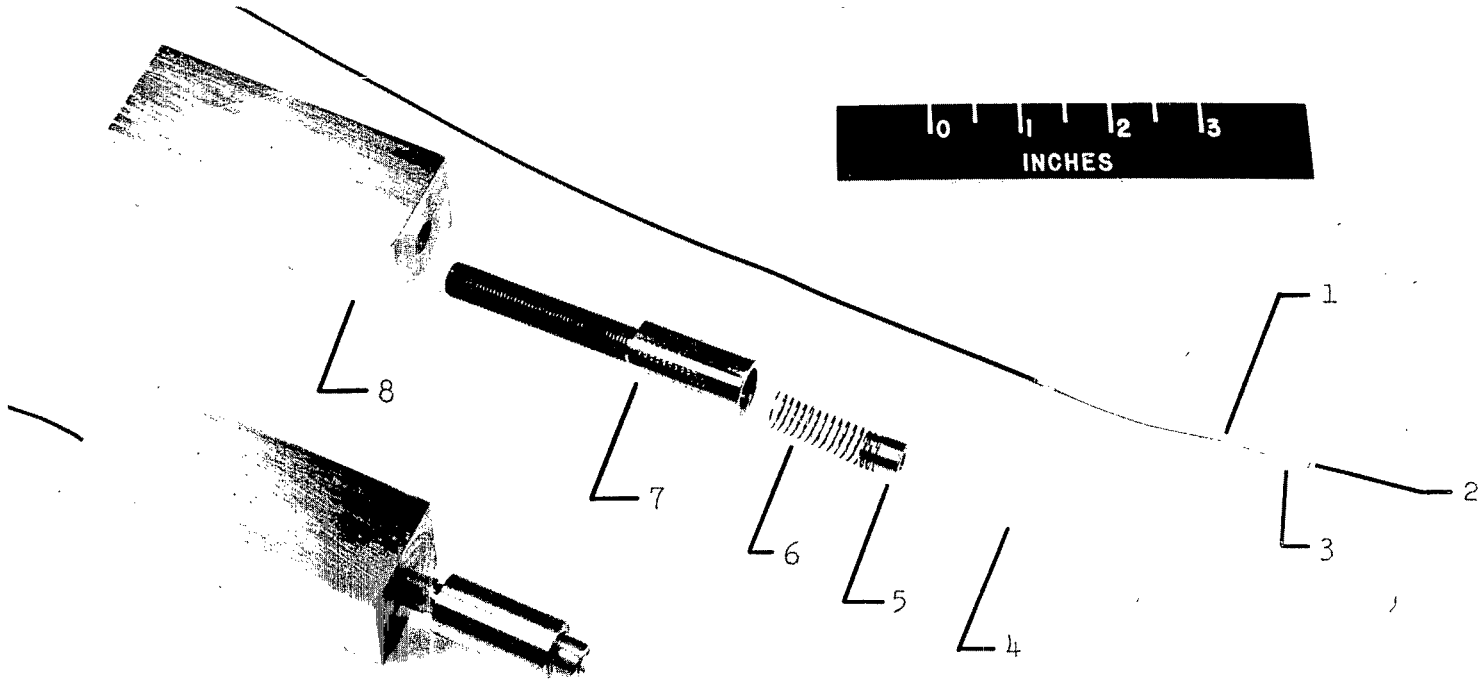

1 Thermocouple wire
2 Thoriated-nickel disk – 3/16 inch (0.476 cm) diameter
3 Fibrous insulation – three layers each 0.040 inch (0.102 cm) thick
4 Ceramic rod
5 Seat
6 Spring
7 Chamber
8 Base

Figure 24.- Spring-loaded thermocouple probe. L-63-3650.1

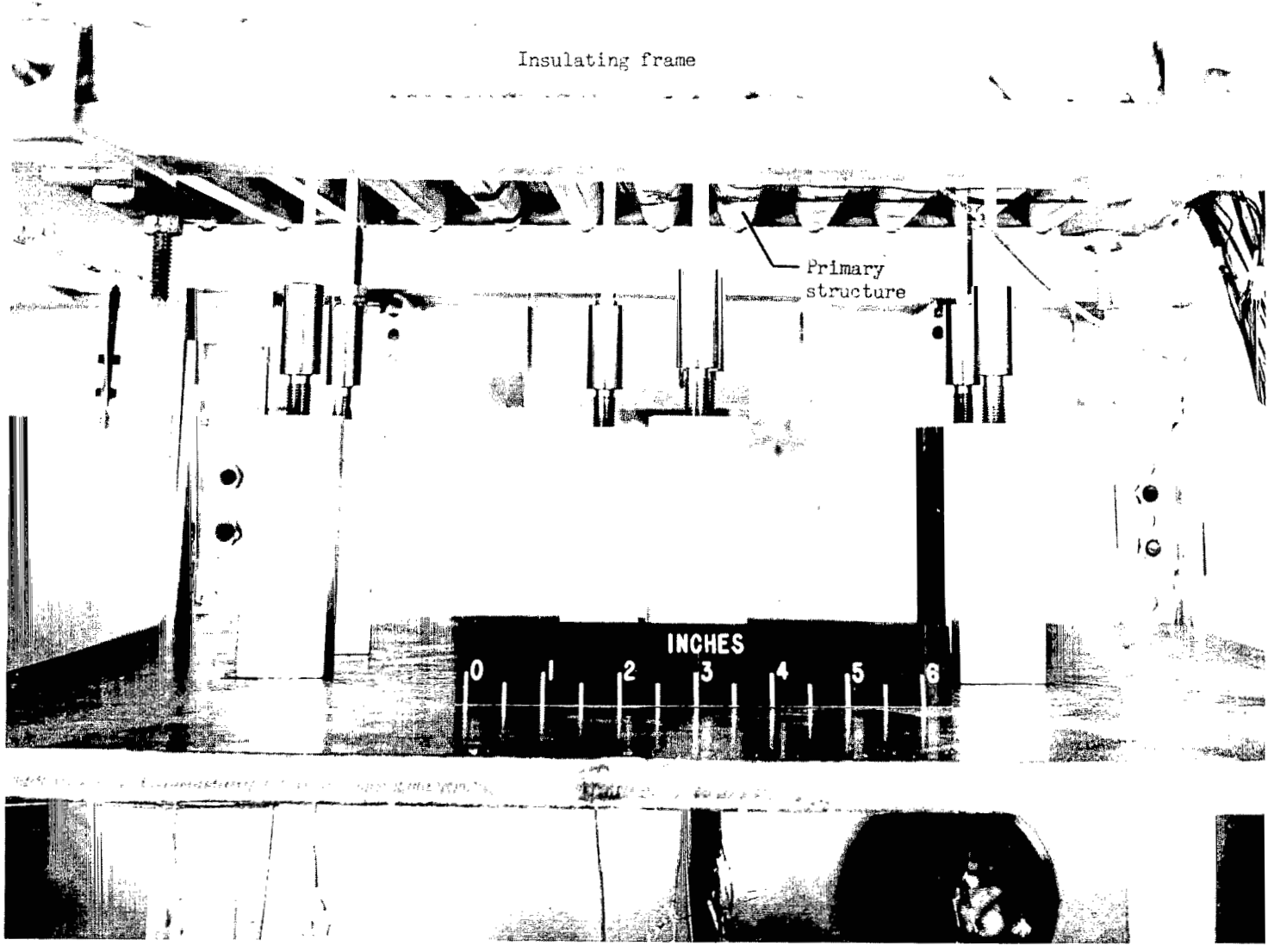

Figure 25.- Thermocouple probes installed for heating test on molybdenum-alloy panel. L-63-3862.1

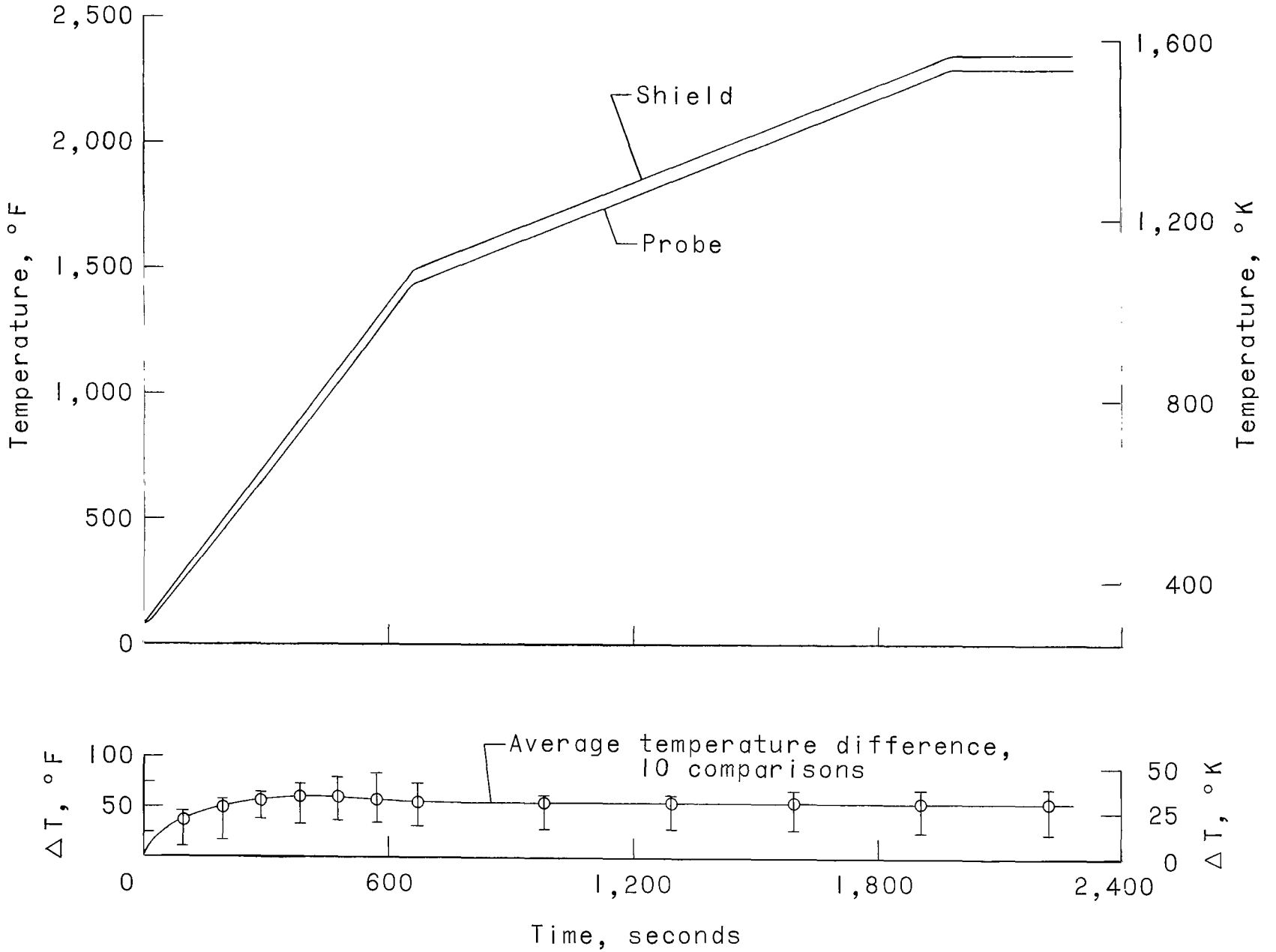

Figure 26.- Probe temperature response compared with shield temperature response. ΔT represents temperature difference.

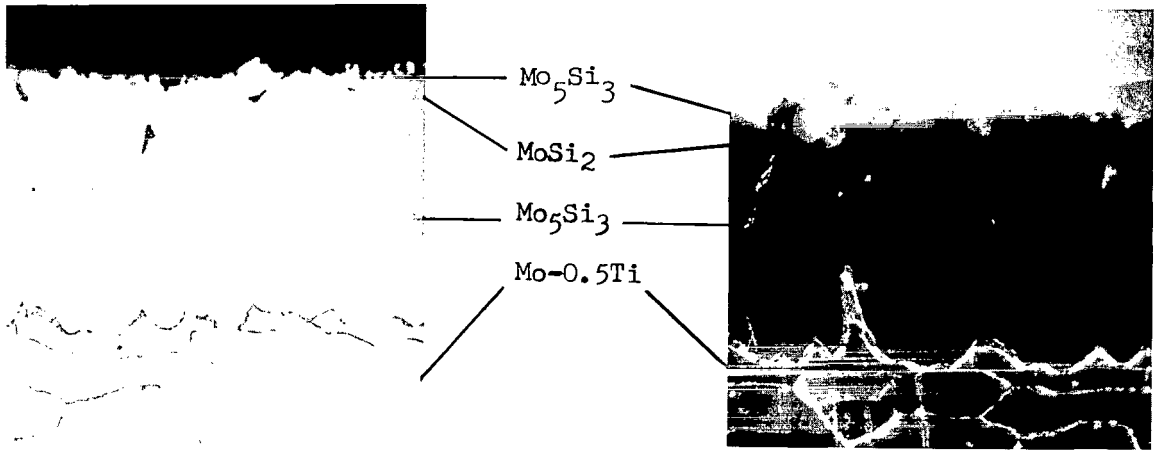

(a) 1.0-hour exposure.

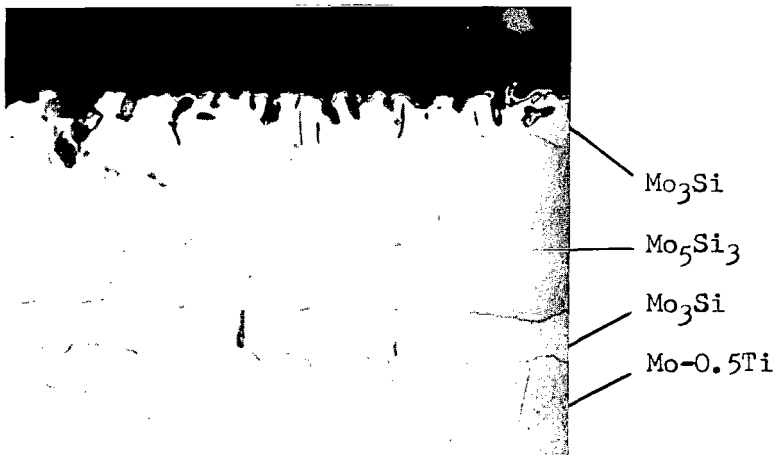

(b) 14-hour exposure. L-64-4733

Figure 27.- Cross-sectional views of silicide-base coating after indicated exposures at 2,900° F (1,866° K) in air. Coating phases were identified by X-ray diffraction. ×500.

"The aeronautical and space activities of the United States shall be conducted so as to contribute . . . to the expansion of human knowledge of phenomena in the atmosphere and space. The Administration shall provide for the widest practicable and appropriate dissemination of information concerning its activities and the results thereof."

—NATIONAL AERONAUTICS AND SPACE ACT OF 1958

NASA SCIENTIFIC AND TECHNICAL PUBLICATIONS

TECHNICAL REPORTS: Scientific and technical information considered important, complete, and a lasting contribution to existing knowledge.

TECHNICAL NOTES: Information less broad in scope but nevertheless of importance as a contribution to existing knowledge.

TECHNICAL MEMORANDUMS: Information receiving limited distribution because of preliminary data, security classification, or other reasons.

CONTRACTOR REPORTS: Technical information generated in connection with a NASA contract or grant and released under NASA auspices.

TECHNICAL TRANSLATIONS: Information published in a foreign language considered to merit NASA distribution in English.

TECHNICAL REPRINTS: Information derived from NASA activities and initially published in the form of journal articles.

SPECIAL PUBLICATIONS: Information derived from or of value to NASA activities but not necessarily reporting the results of individual NASA-programmed scientific efforts. Publications include conference proceedings, monographs, data compilations, handbooks, sourcebooks, and special bibliographies.

Details on the availability of these publications may be obtained from:

SCIENTIFIC AND TECHNICAL INFORMATION DIVISION

NATIONAL AERONAUTICS AND SPACE ADMINISTRATION

Washington, D.C. 20546